NASA/TM—2008-215149

Fuel Cell Thermal Management Through Conductive Cooling Plates

Anthony J. Colozza
Analex Corporation, Cleveland, Ohio

Kenneth A. Burke
Glenn Research Center, Cleveland, Ohio

May 2008

NASA STI Program . . . in Profile

Since its founding, NASA has been dedicated to the advancement of aeronautics and space science. The NASA Scientific and Technical Information (STI) program plays a key part in helping NASA maintain this important role.

The NASA STI Program operates under the auspices of the Agency Chief Information Officer. It collects, organizes, provides for archiving, and disseminates NASA's STI. The NASA STI program provides access to the NASA Aeronautics and Space Database and its public interface, the NASA Technical Reports Server, thus providing one of the largest collections of aeronautical and space science STI in the world. Results are published in both non-NASA channels and by NASA in the NASA STI Report Series, which includes the following report types:

- TECHNICAL PUBLICATION. Reports of completed research or a major significant phase of research that present the results of NASA programs and include extensive data or theoretical analysis. Includes compilations of significant scientific and technical data and information deemed to be of continuing reference value. NASA counterpart of peer-reviewed formal professional papers but has less stringent limitations on manuscript length and extent of graphic presentations.

- TECHNICAL MEMORANDUM. Scientific and technical findings that are preliminary or of specialized interest, e.g., quick release reports, working papers, and bibliographies that contain minimal annotation. Does not contain extensive analysis.

- CONTRACTOR REPORT. Scientific and technical findings by NASA-sponsored contractors and grantees.

- CONFERENCE PUBLICATION. Collected papers from scientific and technical conferences, symposia, seminars, or other meetings sponsored or cosponsored by NASA.

- SPECIAL PUBLICATION. Scientific, technical, or historical information from NASA programs, projects, and missions, often concerned with subjects having substantial public interest.

- TECHNICAL TRANSLATION. English-language translations of foreign scientific and technical material pertinent to NASA's mission.

Specialized services also include creating custom thesauri, building customized databases, organizing and publishing research results.

For more information about the NASA STI program, see the following:

- Access the NASA STI program home page at *http://www.sti.nasa.gov*

- E-mail your question via the Internet to *help@sti.nasa.gov*

- Fax your question to the NASA STI Help Desk at 301–621–0134

- Telephone the NASA STI Help Desk at 301–621–0390

- Write to:
  NASA Center for AeroSpace Information (CASI)
  7115 Standard Drive
  Hanover, MD 21076–1320

NASA/TM—2008-215149

Fuel Cell Thermal Management Through Conductive Cooling Plates

Anthony J. Colozza
Analex Corporation, Cleveland, Ohio

Kenneth A. Burke
Glenn Research Center, Cleveland, Ohio

National Aeronautics and
Space Administration

Glenn Research Center
Cleveland, Ohio 44135

May 2008

Level of Review: This material has been technically reviewed by technical management.

Available from

NASA Center for Aerospace Information
7115 Standard Drive
Hanover, MD 21076–1320

National Technical Information Service
5285 Port Royal Road
Springfield, VA 22161

Available electronically at http://gltrs.grc.nasa.gov

Fuel Cell Thermal Management Through Conductive Cooling Plates

Anthony J. Colozza
Analex Corporation
Cleveland, Ohio 44135

Kenneth A. Burke
National Aeronautics and Space Administration
Glenn Research Center
Cleveland, Ohio 44135

Abstract

An analysis was performed to evaluate the concept of utilizing conductive cooling plates to remove heat from a fuel cell stack, as opposed to a conventional internal cooling loop. The potential advantages of this type of cooling system are reduced stack complexity and weight and increased reliability through the reduction of the number of internal fluid seals. The conductive cooling plates would extract heat from the stack transferring it to an external coolant loop. The analysis was performed to determine the required thickness of these plates. The analysis was based on an energy balance between the thermal energy produced within the stack and the heat removal from the cooling plates. To accomplish the energy balance the heat flow into and along the plates to the cooling fluid was modeled. Results were generated for various numbers of cells being cooled by a single cooling plate. The results provided cooling plate thickness, mass and operating temperature of the plates. It was determined that utilizing high conductivity pyrolitic graphite cooling plates can provide a specific cooling capacity (W/kg) equivalent to or potentially greater then a conventional internal cooling loop system.

Introduction

A proton exchange membrane (PEM) fuel cell is essentially a solid-state device consisting of various layers of materials, to electrochemically produce electricity through the combination of hydrogen and oxygen, given by equations (1) and (2). The fuel cell stack consists of a number of these individual flat-plate layers or cells where the electrochemical process occurs. The overall efficiency in converting the reactants to electricity within these cells is on the order of 50 percent. This means that around half of the energy produced in the combining of hydrogen and oxygen is released as heat. For the fuel cell to function properly this heat must be removed from the fuel cell stack to maintain its required operating temperature.

$$\text{Anode Reaction:} \qquad 2H_2 \rightarrow 4H^+ + 4e^- \tag{1}$$

$$\text{Cathode Reaction:} \qquad O_2 + 4e^- + 4H^+ \rightarrow 2H_2O + heat \tag{2}$$

In a PEM stack this heat is generated at the membrane electrode assembly (MEA) where the electro-chemical process takes place. To prevent an excessive rise in temperature within the stack the heat generated must then be transferred from the MEA to a cooling fluid (either gas or liquid) and removed from the system.

For the MEA to function a supply of hydrogen and oxygen (or air) must be brought to the anode and cathode sides respectively. Also an electrical connection must be made between the anode of one cell and the cathode of the next in order to electrically connect the cells. This gas flow and electrical connection is accomplished through a bipolar plate. This plate is situated between the anode of one cell and the cathode of the next. It is constructed of a conductive material such as graphite or stainless steel to provide the electrical connection between the cells. It also has passages on both sides, which provide an even

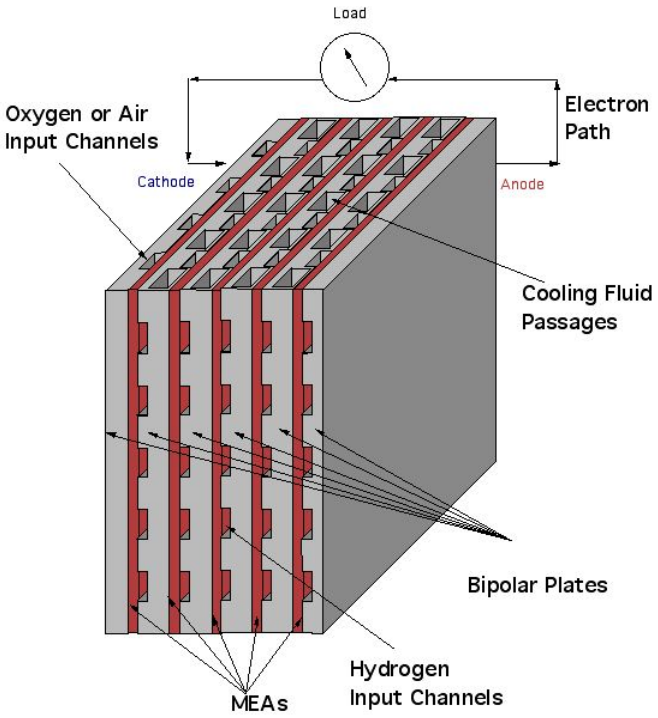

Figure 1.—Basic cell stack assembly diagram.

distribution of hydrogen and oxygen to the anode and cathode surfaces respectively. A simplified diagram of this cell stack assembly is shown in figure 1.

The MEAs and bipolar cells must be sealed together in order to prevent gas from leaking from the stack. Because of the extensive and intricate gas flow within the stack, sealing against leaks is a significant task. This is usually accomplished through the use of gaskets or other sealing material. These sealing materials, the coatings on the MEA and the polymer membrane itself limit the maximum operational temperature of the stack. A critical aspect of a fuel cell's operation is the ability to maintain its temperature within a range suitable for its operation. The operating temperature for a proton exchange membrane (PEM) fuel cell is usually within the range of 30 to 100 °C (ref. 1).

Most conventional PEM fuel cell designs utilize the bipolar plate as a means of cooling the stack. This is accomplished by placing additional passages within the bipolar plate, separate from the reactant gas passages. Water or air is passed through these passages to directly cool the MEA. For lower power hydrogen-air fuel cells, generally those that produce 100 W or less, the reactant air can be used as a means of cooling the stack. Above this power level, the reactant air and the cooling air must be separated (ref. 1). At these higher power levels separate cooling passages through the bipolar plates, as shown in figure 1, are used to pass the coolant air. This type of cooling is employed in the Ballard Nexa 1 kW fuel cell. The Nexa fuel cell is shown in figure 2 where the cooling passages can be easily seen in the bipolar plates.

Above approximately 2 kW in output power, water or some other type of liquid cooling fluid is utilized to cool the fuel cell stack instead of air. Similar cooling passages through the bipolar plates are also utilized with the liquid-cooled fuel cell stack as with the air-cooled stack (ref. 1).

As the power level of the fuel cell increases, the coolant passage will also need to increase to accommodate the added heat flux. This in turn increases the stack volume. With the recent advancements in highly thermally conductive carbon fiber plates as well as the development of flat plate heat pipes an alternate means of cooling the fuel cell stack may be possible. This alternate approach is to utilize these types of materials to conduct heat out of the stack where it can be removed by a separate cooling flow. The integration of this type of cooling plate is illustrated in figure 3. Because of its placement between bipolar plates heat from the MEA will be conducted through the bipolar plate to the conductive plate and then out to a cooling loop.

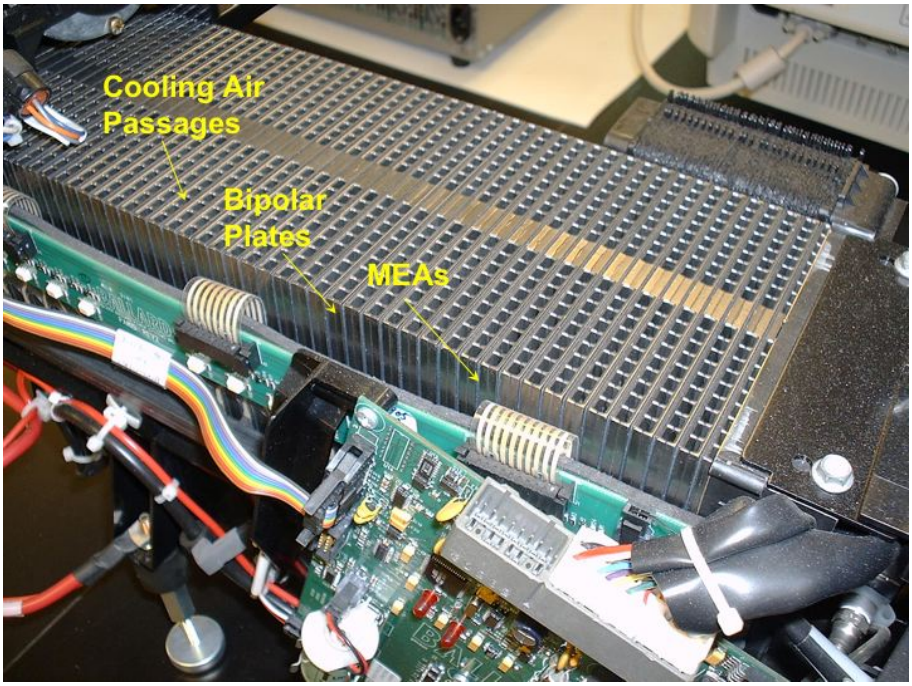

Figure 2.—Ballard Nexa fuel cell stack.

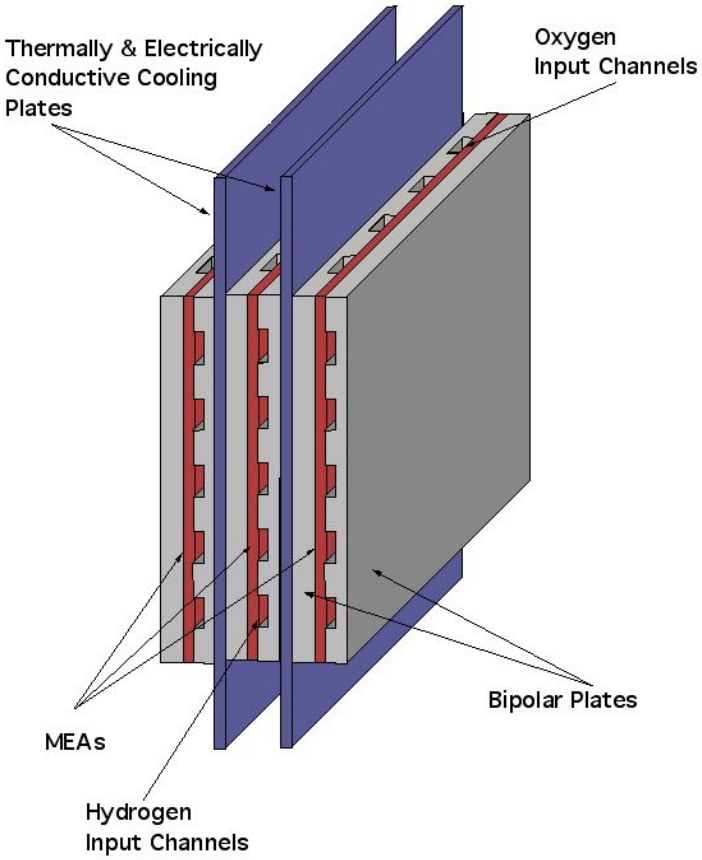

Figure 3.—Integrated cooling plate between modified bipolar plates.

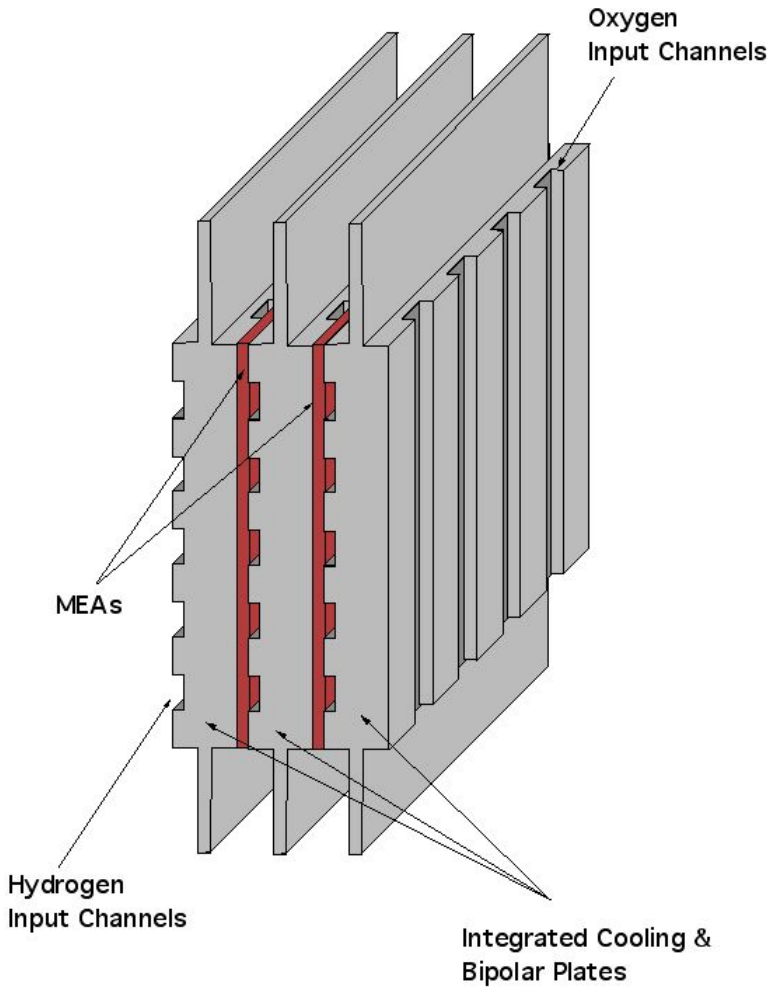

Figure 4.—Integrated cooling and bipolar plate concept.

A more refined alternative to this independent cooling plate design is to integrate the bipolar plate and cooling plate into one unit, as shown in figure 4. The ability to accomplish this would be dependent on the type of material that the cooling plate is constructed from. The material would need to be able to be easily machined or formed to accommodate the channels needed for the reactant gas passages as well as be compatible with the reactants.

The potential advantages of this type of conductive plate cooling scheme are in reducing the stack complexity, mass, and volume. Eliminating the need for cooling passages within the cells and making the cooling system external to the fuel cell stack can achieve this. This arrangement can potentially reduce the auxiliary components needed to operate the fuel cell, reduce mass if lightweight cooling plates are utilized as well as improve reliability by eliminating some of the internal seals within the stack. Also this approach could reduce the complexity of the bipolar plate, which in turn could potentially reduce the fuel cell manufacturing cost. An illustration of the differences in required components between a dedicated conventional cooling loop system and the external cooling system is shown in figure 5.

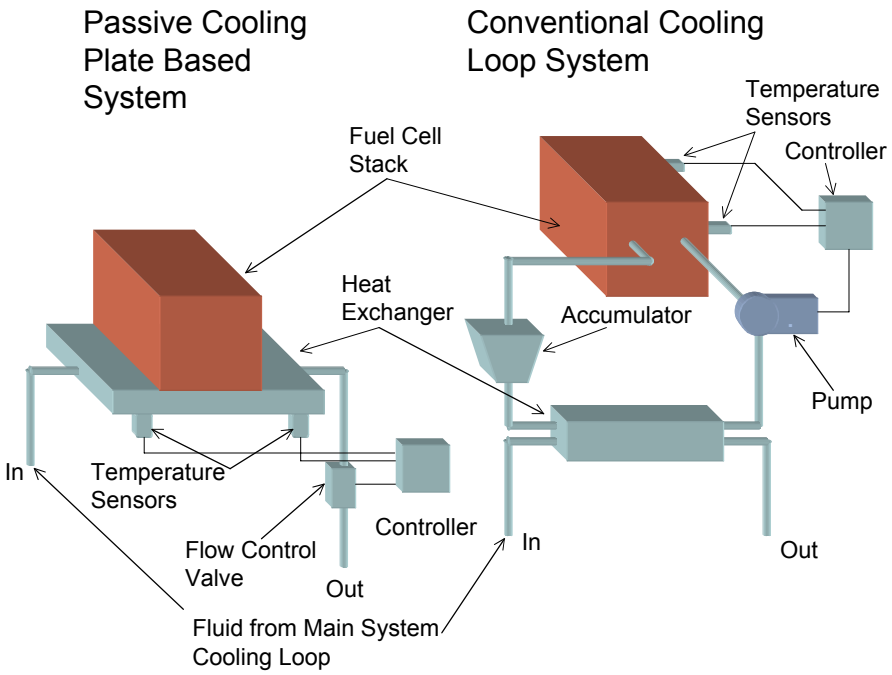

Figure 5.—Comparison of components between a conventional dedicated internal cooling system and the cooling plated based external cooling system.

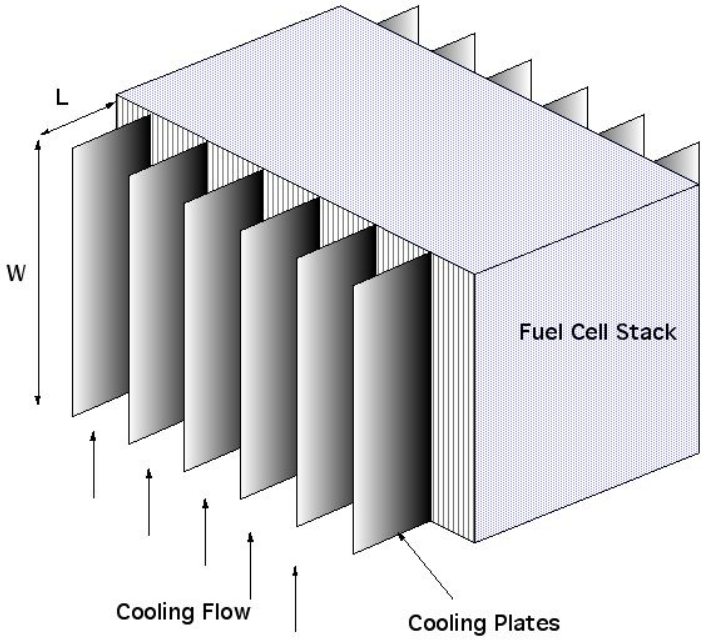

Figure 6.—Fuel cell stack with cooling plates.

Analysis

Cooling Plate Analysis

The removal of heat from a fuel cell stack can be accomplished by a series of conductive plates between each or some larger grouping of the cells that comprise the stack. This configuration is shown in figure 6. These plates will extend out beyond the stack to conduct the excess heat produced through the operation of the fuel cell to an external fluid for removal from the system. The initial sizing of these plates

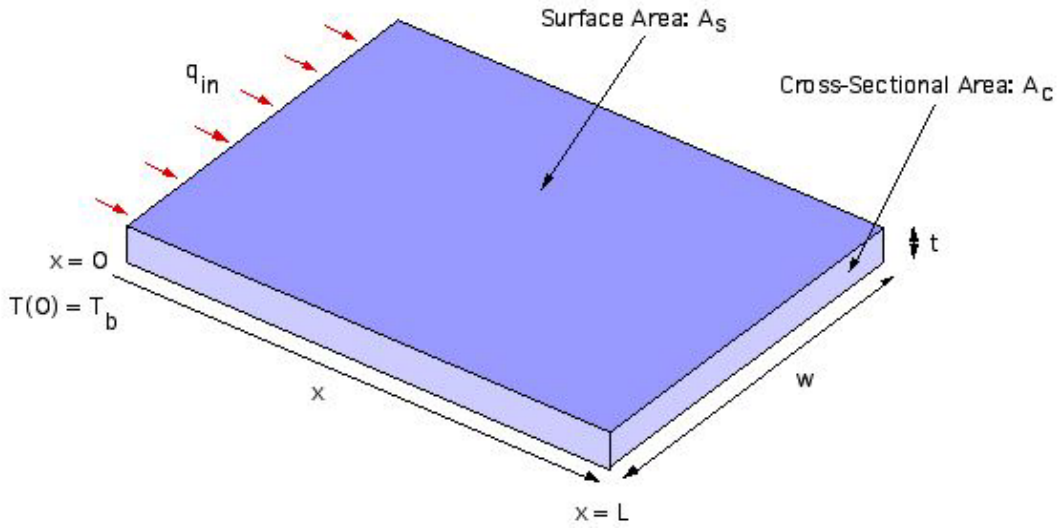

Figure 7.—Cooling fin geometry diagram.

can be accomplished through an energy balance between the heat generated within the stack and the heat extracted by the external cooling fluid. To set up this energy balance the heat flow into and along the plates and to the cooling fluid must be modeled.

The first step in sizing the cooling plates is to determine the heat transfer to the surrounding cooling flow. This is accomplished by starting with the basic one-dimensional conduction equation for an extended surface with convective heat transfer from the surface. This is given by equation (3) (ref. 1). This equation is derived from the conservation of energy along the extended surface. It is based on the geometry of the plate (cross-sectional area A_c and surface area A_s) as well as plate conductivity (k) and the cooling fluid convection coefficient (h) and temperature (T_f).

$$\frac{d^2T}{dx^2} + \left(\frac{1}{A_c}\frac{dA_c}{dx}\right)\frac{dT}{dx} - \left(\frac{1h}{A_c k}\frac{dA_s}{dx}\right)(T - T_f) = 0 \tag{3}$$

A diagram of the cooling plate geometry is given in figure 7. This figure shows the portion of the plate that is outside of the fuel cell stack, as seen in figure 1. All heat transfer to this part of the plate occurs through conduction down its length. From this geometry it can be seen that the cooling plate is assumed to have a constant cross sectional area along the length. Therefore the second term in equation (3) will be zero.

Based on this geometry equation (3) can be placed into the form of a linear, homogenous second order differential Equation (given by equations (4) to (6)) of which a general solution is known.

$$\frac{d^2\theta(x)}{dx^2} - m^2\theta(x) = 0 \tag{4}$$

where

$$m^2 = \frac{(2w + 2t)h}{wtk} \tag{5}$$

$$\theta(x) = T(x) - T_f \tag{6}$$

This general solution to equation (4) is given by equation (7) (ref. 3) where the constants (C_1 and C_2) are determined through the boundary conditions for the plate dictated by the plate geometry, shown in figure 7, and fuel cell operational conditions.

$$\theta(x) = C_1 e^{mx} + C_2 e^{-mx} \tag{7}$$

The fuel cell stack operational temperature (T_0) sets the first boundary condition. This operating temperature can be considered a constant and must be maintained in order to prevent damage to the fuel cell. This initial boundary condition sets the temperature at the base of the fin ($x = 0$) and is given by equation (8).

$$\theta(x)\big|_{x=0} = T_0 - T_f = \theta_0 \tag{8}$$

Substituting equation (7) into this boundary condition relationship yields a relation for the constants given by equation (9).

$$\theta_0 = C_1 + C_2 \tag{9}$$

The next boundary condition relates to the total heat flow out of the fin. The heat flow into the fin from the stack must be equal to the heat removed from the fin by convection. Equation (10) represents this energy balance between the heat conduction down the fin and heat removal from the fin through convection at the tip of the fin ($x = L$).

$$-kwt\frac{dT(x)}{dx}\bigg|_{x=L} = hwt(T(L) - T_f) \tag{10}$$

Where for a constant cooling fluid temperature (T_f):

$$\theta(L) = T(L) - T_f \;\therefore \frac{d\theta(x)}{dx}\bigg|_{x=L} = \frac{dT(x)}{dx}\bigg|_{x=L} \tag{11}$$

Substituting equation (11) into (10) yields equation (12).

$$-k\frac{d\theta(x)}{dx}\bigg|_{x=L} = h\theta(L) \tag{12}$$

The solution given by equation (7) must now be substituted into the boundary relation given by equation (12). To accomplish this the derivative of equation (7) must be taken with respect to x. This derivative is given by equation (13) and the resulting equation after substituting and rearranging is given by equation (14).

$$\frac{d\theta(x)}{dx}\bigg|_{x=L} = mC_1 e^{ml} - mC_2 e^{-ml} \tag{13}$$

$$C_1\left(\frac{mk}{h} + 1\right)e^{ml} + C_2\left(1 - \frac{mk}{h}\right)e^{-ml} = 0 \tag{14}$$

Equations (9) and (14) can then be solved to provide expressions for the constants C_1 and C_2, these expressions are given by equations (15) and (16), respectively for these boundary conditions.

$$C_1 = \theta_b - \frac{\theta_b e^{ml}\left(\frac{mk}{h}+1\right)}{\left(e^{-ml}\left(\frac{mk}{h}-1\right)+e^{ml}\left(\frac{mk}{h}+1\right)\right)} \tag{15}$$

$$C_2 = \frac{\theta_b e^{ml}\left(\frac{mk}{h}+1\right)}{\left(e^{-ml}\left(\frac{mk}{h}-1\right)+e^{ml}\left(\frac{mk}{h}+1\right)\right)} \tag{16}$$

Substituting these expressions for the constants into equation (7) and utilizing the definitions of the hyperbolic sine and cosine (ref. 4), given in equations (17) and (18), respectively yields a relationship for the temperature along the plate $T(x)$ given in equation (19).

$$\sinh x = \frac{e^{x} - e^{-x}}{2} \tag{17}$$

$$\cosh x = \frac{e^{x} + e^{-x}}{2} \tag{18}$$

$$T(x) = (T_o - T_f)\frac{\cosh\left(\sqrt{\frac{(2w+2t)h}{wtk}}(L-x)\right) + \sqrt{\frac{wth}{(2w+2t)k}}\sinh\left(\sqrt{\frac{(2w+2t)h}{wtk}}(L-x)\right)}{\cosh\left(\sqrt{\frac{(2w+2t)h}{wtk}}L\right) + \sqrt{\frac{wth}{(2w+2t)k}}\sinh\left(\sqrt{\frac{(2w+2t)h}{wtk}}L\right)} + T_f \tag{19}$$

The next step is to determine an equation for the heat flow within the fin. Utilizing Fourier's law, given by equation (20), and substituting in equation (19) for the temperature function results in an expression for the heat flow in the portion of the cooling plate that extends beyond the fuel cell stack over which the cooling fluid flows. This is given by equation (21).

$$q = -ktw\left.\frac{dT}{dx}\right|_{x=0} \tag{20}$$

$$q = (T_0 - T_f)\sqrt{(2w+2t)hkwt}\,\frac{\sinh\left(\sqrt{\frac{(2w+2t)h}{wtk}}L\right) + \sqrt{\frac{wth}{(2w+2t)k}}\cosh\left(\sqrt{\frac{(2w+2t)h}{wtk}}L\right)}{\cosh\left(\sqrt{\frac{(2w+2t)h}{wtk}}L\right) + \sqrt{\frac{wth}{(2w+2t)k}}\sinh\left(\sqrt{\frac{(2w+2t)h}{wtk}}L\right)} \tag{21}$$

For a known heat flow (q) and desired temperature (T_0) of the fuel cell, equation (21) can be iterated upon to determine the required plate thickness to meet the specified heat transfer requirements.

To determine the required plate thickness the fuel cell temperature, plate thermal conductivity, cooling fluid convective heat transfer coefficient, heat flow into the plate and plate dimensions (length and width) must be specified.

The conductivity of the plate will dependent on the plate material. Some examples of thermal conductivities of various materials is given in table 1. The thermal conductivity of a material will change depending on its temperature. However, this variation with temperature, within the operating range of the fuel cell, is minimal and for this analysis can assume to be negligible.

TABLE 1.—THERMAL CONDUCTIVITY OF SELECTED MATERIALS (REFS. 1 AND 5)

Material	Thermal conductivity, W/m K	Density, kg/m^3
Aluminum	237	2,702
Beryllium	218	1,850
Copper	398	8,933
Gold	315	19,300
Silver	427	10,500
Diamond	2300	3,500
Pyrolytic graphite (parallel to fibers)	1950	2,210
Pyrolytic graphite (perpendicular to fibers)	5.70	2,210
Pyrolytic graphite plate	1200	2,210
Silicon carbide	490	3,160
Graphite plate	152	1,800
Metal carbon composite	800	4,910

The convective heat transfer of the plate to the surrounding fluid (either a liquid or gas) will depend on the convective heat transfer coefficient of the fluid. The range of coefficient values for various fluids is given in table 2.

TABLE 2.—TYPICAL CONVECTIVE HEAT TRANSFER COEFFICIENTS (REF. 1)

Type of convection	Typical convection coefficient range, W/m^2K
Free Convection of a Gas	2 to 25
Free Convection of a Liquid	50 to 1000
Forced Convection of a Gas	25 to 250
Forced Convection of a Liquid	50 to 20,000
Convection with Phase Change	2,500 to 100,000

The heat flow into the plate is based on the operating characteristics of the fuel cell and the number of cells transferring heat to a given plate. For the initial analysis it is assumed that each cell in the fuel cell stack has a single heat transfer plate. Also based on the geometry shown in figure 6, the heat produced by the cell is distributed evenly to the two edges of the plate that extend beyond the fuel cell body. Therefore the heat flow that must be dissipated by the plate that extends from the stack, as shown in figure 7 and represented by equation (21), is also given by equation (22) for the specific cell operating voltage (V), current density (j), height (h), width (w) and efficiency (η_{fc}) of the fuel cell stack.

$$q = \frac{jVwh}{2}\left(\frac{1}{\eta_{fc}} - 1\right) \tag{22}$$

The initial or baseline fuel cell operating conditions and geometry used to solve for the required plate thickness is given in table 3.

Utilizing the baseline operational values, given in table 3, the required plate thickness to accommodate the heat transfer from the extended surface was calculated for a range of convective heat transfer coefficients (from 20 to 2,000 W/m^2K) and plate thermal conductivities (from 200 to 2,000 W/mK). The required plate thickness was determined through an iterative process utilizing equations (21) and (22). The results from this portion of the analysis were generated to show how the

TABLE 3.—BASELINE FUEL CELL
OPERATING PROPERTIES

Property	Value
Current density (j)	0.28 A/cm^2
Cell voltage (V)	0.5 V
Fuel cell width (w)	15 cm
Fuel cell height (h)	15 cm
Fuel cell efficiency (η_{fc})	50%
Fuel cell operating temperature (T_0)	353 K
Cooling fluid temperature (T_f)	298 K
Output power per cell	31.5 W

variables affected the heat transfer from the portion of the cooling plate extending beyond the stack. These results are shown in figures 8 to 13.

Figures 8 and 9 illustrate the required plate thickness needed to maintain the required stack operational temperature with the plates extending 3 and 6 cm beyond the fuel cell body, respectively. From these figures it can be seen that plate thickness will decrease with both increasing plate conductivity and cooling fluid convective coefficient. The largest reduction in thickness can be seen with increases in plate conductivity up to approximately 500 W/m K where the overall heat flux becomes limited by convection heat transfer. Beyond this point the gain due to increasing conductivity is reduced. This is in contrast to the effect of increasing the convective coefficient. Increases in convective coefficient will produce a significant and continuous reduction in the required plate thickness over the full range of plate conductivities. This can be seen by the fairly constant spacing between the thickness curves shown in the figures. Also extending the plate length from 3 to 6 cm produced thinner plates but only had a significant effect at low convective coefficient values, below 60 W/m^{2}K.

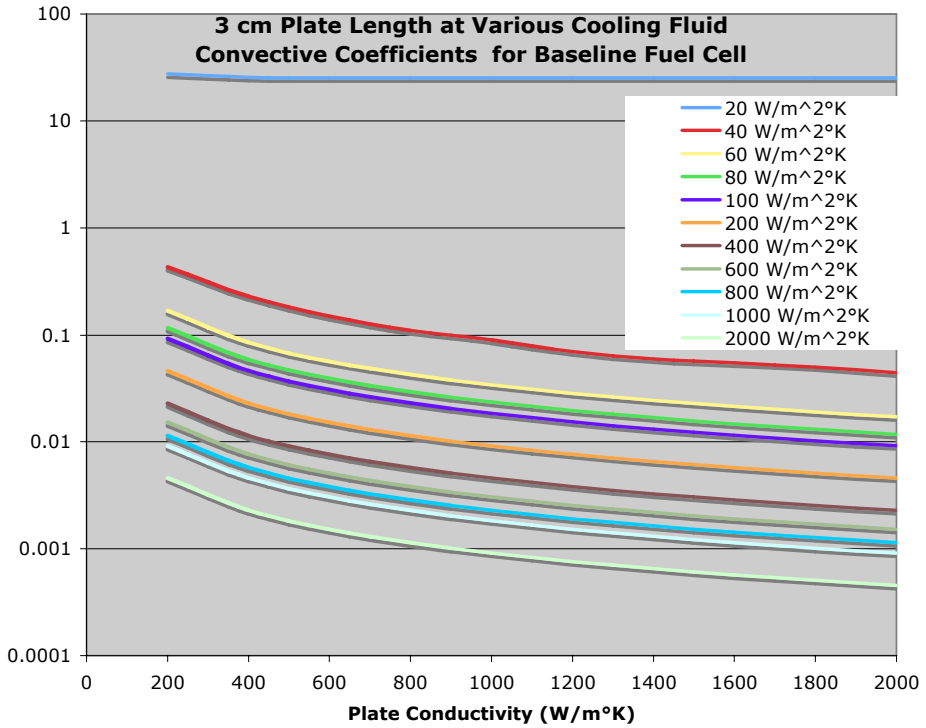

Figure 8.—Required plate thickness for maintaining stack temperature with a 3 cm fin versus plate thermal conductivity for various cooling fluid convective coefficients (baseline fuel cell).

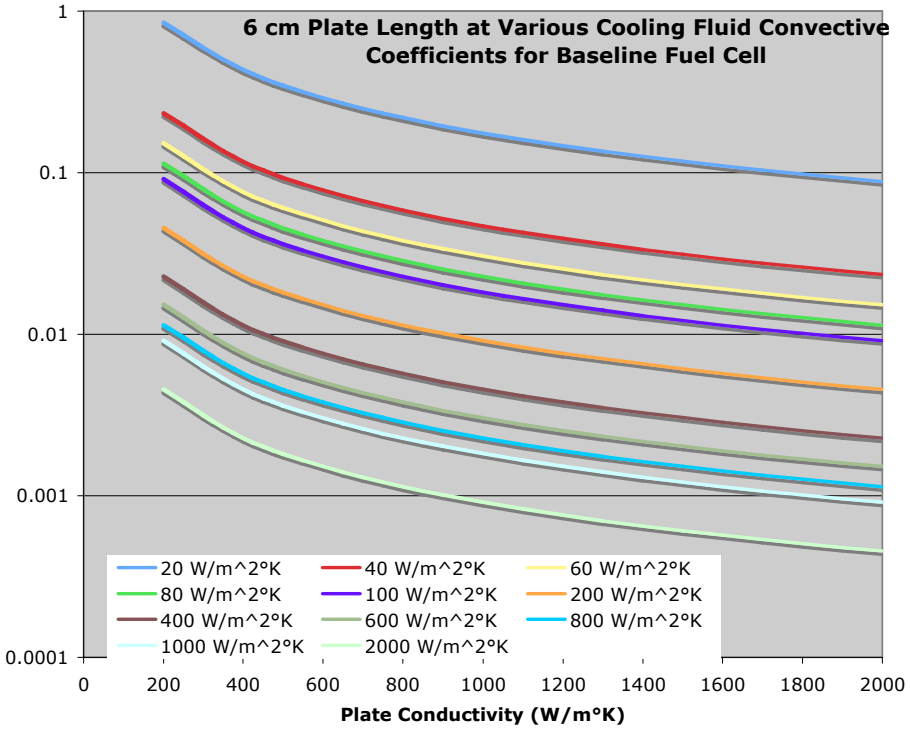

Figure 9.—Required plate thickness for maintaining stack temperature with a 6 cm fin versus plate thermal conductivity for various cooling fluid convective coefficients (baseline fuel cell).

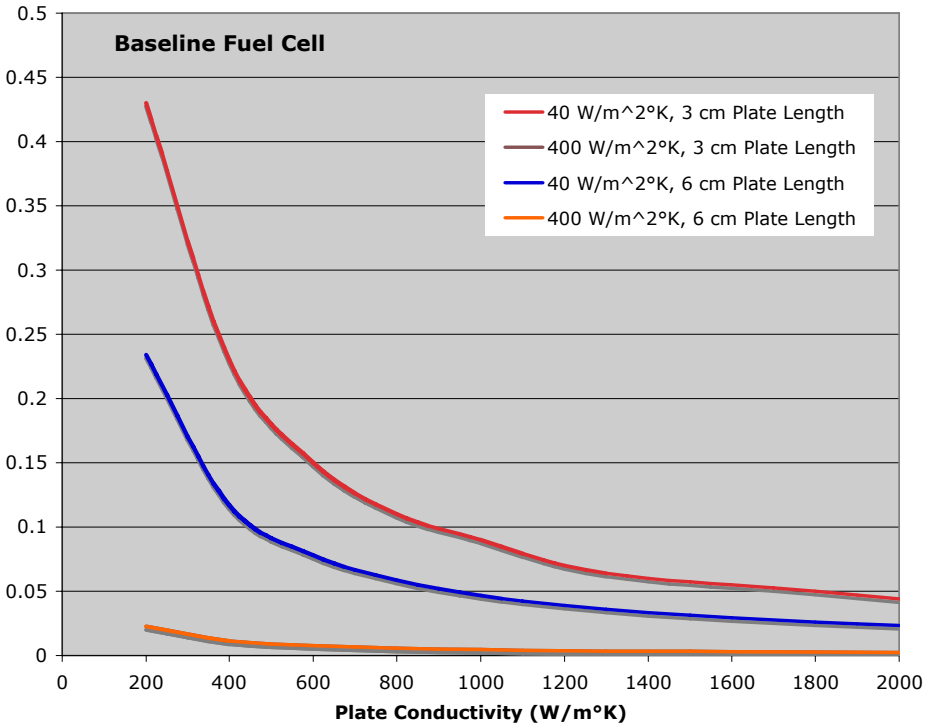

Figure 10.—Plate thickness versus conductivity for variations in convective coefficient and plate length (baseline fuel cell).

In order to display all of the data, figures 8 and 9 utilize a log scale for the Y axis. The dependency of the plate thickness on conductivity, convection coefficient and plate length can be better illustrated through a linear plot, as given in figure 10. This figure shows thickness curves for a convection coefficient of between 40 and 400 W/m^2 K for both plate lengths of 3 and 6 cm. At the low convection coefficient value (40 W/m^2 K), the increase in plate conductivity produced a significant reduction in plate thickness. At the higher convective coefficient value (400 W/m^2 K) there was little change in plate thickness with an increase in conductivity. Also, for the lower value of convection coefficient, an increase in plate length produced a reduction in plate thickness. However, at the higher convective coefficient, there was no change in thickness due to a change in plate length from 3 to 6 cm (both of the 400 W/m^{2}K curves are similar and appear on top of one another in figure 10).

The figures given above demonstrate that the convective coefficient has the greatest effect on reducing the plate thickness. If a fluid with a low convective coefficient is utilized then increasing the plate conductivity and length can reduce the required plate thickness. At lower plate conductivities, below 500 W/m K, there is a significant reduction in plate thickness with increasing plate conductivity. Beyond this point the reduction in plate thickness seen as the plate conductivity increases begins to level off.

The analysis and results shown above were generated based on the operating properties given in table 3. It was assumed that there would be one conductive plate per cell and that heat generated by the cell would be dissipated by the extension of the plate beyond the fuel cell stack, as seen in figure 6. Since the plate extended from two sides of the stack, each extended portion of the plate, shown in figure 7, would dissipate half of the heat generated by the cell.

To potentially reduce mass as well as the number of plates that would need to be installed, the analysis was extended to look at the required plate thickness needed to dissipate heat from multiple cells. This initial analysis did not account for the variation in temperature within the stack itself. The heat load per cell, based on the operating properties given in table 3, is 31.5 W. Therefore each plate extension would need to dissipate half of that or 15.75 W per cell. The required cooling plate thickness for various convective coefficients at different heat loads was calculated. These results are shown in figures 11 to 13 for plate conductivities of 400, 800, and 1,200 W/m K, respectively.

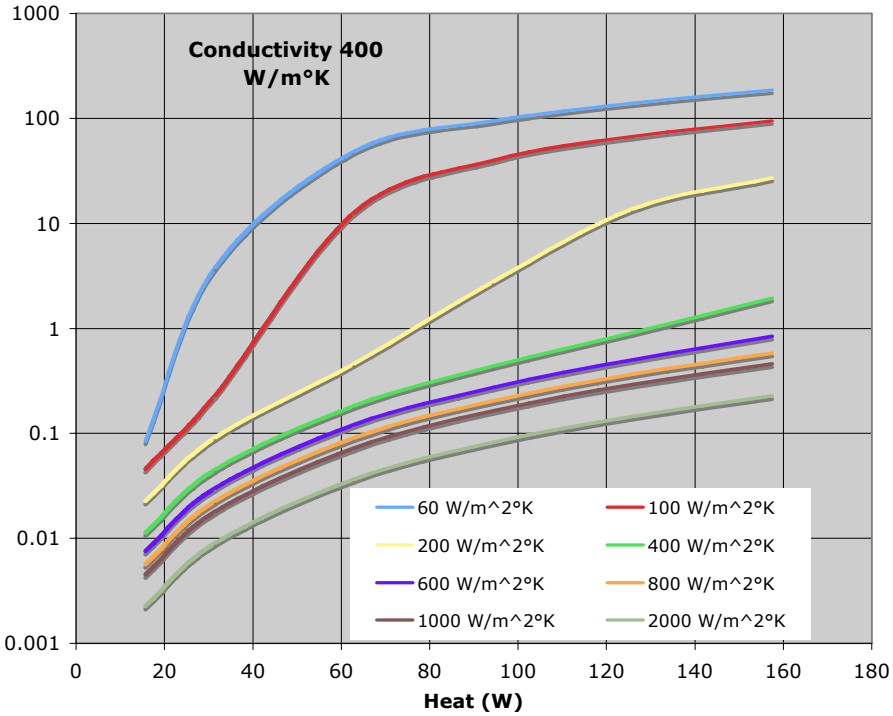

Figure 11.—Cooling plate thickness versus heat load for various convective coefficients with a plate conductivity of 400 W/m K (baseline fuel cell).

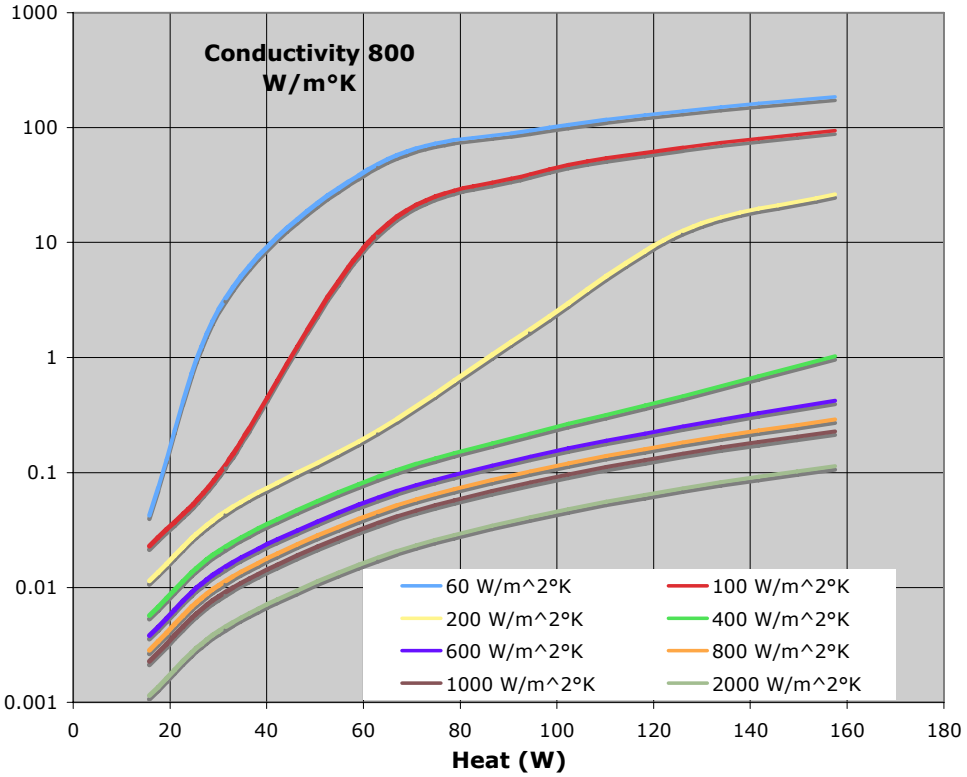

Figure 12.—Cooling plate thickness versus heat load for various convective coefficients with a plate conductivity of 800 W/m K (baseline fuel cell).

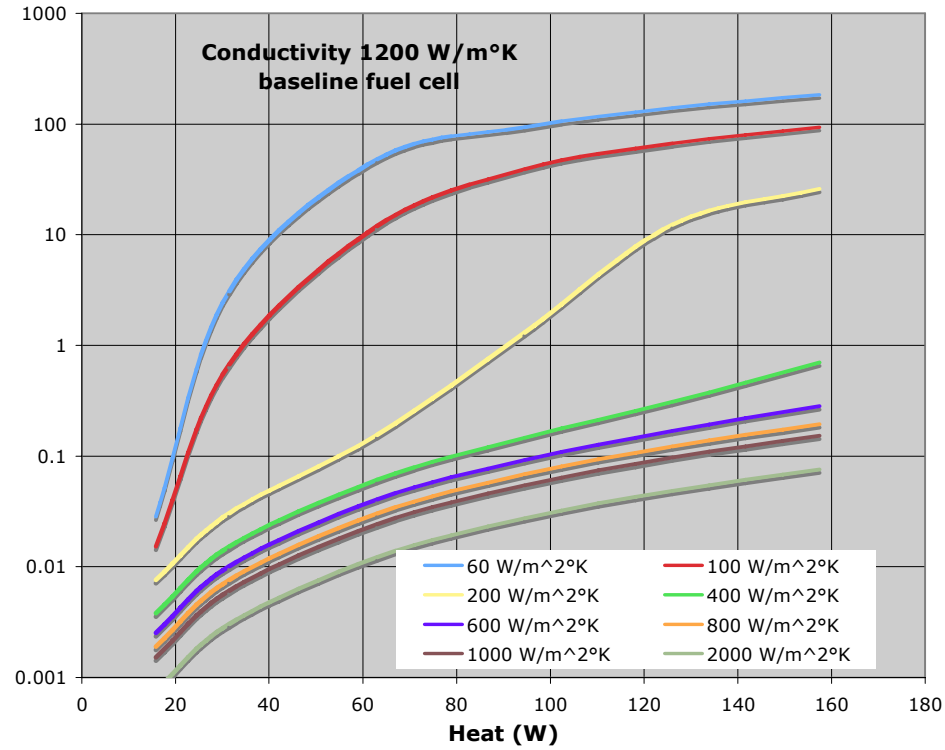

Figure 13.—Cooling plate thickness versus heat load for various convective coefficients with a plate conductivity of 1,200 W/m K (baseline fuel cell).

From these figures it can be seen that increasing the heat load on each cooling plate can significantly increase its required thickness. Increasing thermal conductivity of the plate does reduce plate thickness somewhat. However, more significant benefits are achieved by increasing the convective coefficient. At convective coefficient values of 400 W/m^2K and above increasing thermal conductivity of the cooling plate provides a more significant benefit in reducing the required plate thickness. This result should be expected. At lower convective coefficient values, the convective coefficient limits the heat transfer and therefore no matter how conductive the cooling plate the cooling fluid can remove only so much heat. As the convective coefficient increases, the thermal conductivity of the plate becomes the limiting factor. Therefore for high convective coefficients, increases in the plate thermal conductivity reduce the required plate thickness.

The data presented in these figures can also be used to show the effect changing the heat load has on the required convective coefficient for a plate of a specified thickness. This is illustrated in figure 14 for a plate with a thickness of 0.1 mm and convective coefficients of 400, 800, and 1200 W/m K. From this figure it can be seen that, for a given size cooling plate, increasing the thermal conductivity of the plate can provide a significant reduction in the required convective coefficient with increasing thermal load on the plate. In other words, if less cooling plates are utilized within the stack then increasing the conductivity of the plates will reduce the required convective coefficient of the cooling fluid and possibly enable the same thickness plates to be utilized thereby reducing the stack mass.

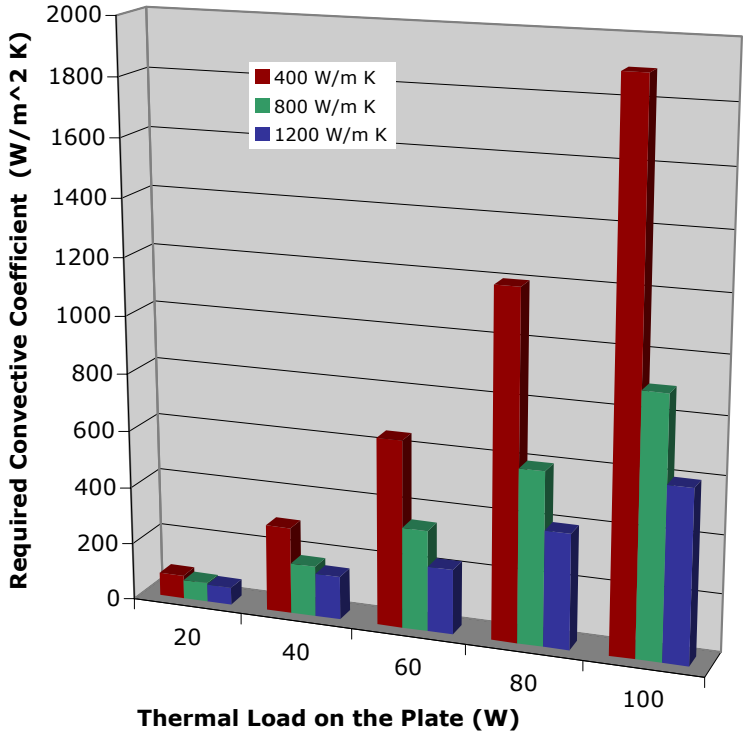

Figure 14.—Required convective coefficient for a 0.1 mm plate thickness and various plate thermal conductivities.

Convective Heat Transfer From the Cooling Plate

The figures shown in the previous section demonstrate the effect that the heat transfer coefficient has on the required plate thickness. The ability to achieve the desired coefficient for a specific plate thickness will depend on the properties of the cooling fluid. Assuming the cooling fluid flow over the plates is as shown in figure 6, the convective heat transfer coefficient can be determined for a given cooling fluid. Depending on the plate spacing, the convective coefficient can be determined based on external flow over

a single plate or internal flow between two plates. Calculations of the convective heat transfer coefficient under both these conditions are given below.

In both cases specific properties of the cooling fluids must be known. Heat transfer coefficients were determined for four different cooling fluids over a range of flow velocities. The cooling fluids considered were; water, air, hydrogen and oxygen. Hydrogen and oxygen were included as potential cooling fluids since they are the reactants utilized by the fuel cell. Because of this there is the potential to also utilize these gasses as the cooling fluid.

Curve fits for the various properties, density (ρ_l), specific heat (c_{pf}), conductivity (k_f) and viscosity (μ_f) (ref. 4), of each of these fluids were generated as a function of temperature (T_f). The curve fits as well as the temperature ranges they are valid within are given in equations (23) to (38).

Water (valid between 273 and 588 K);

$$\rho_f = -404.87 + 14.121T_f - 0.050664T_f{}^2 + 7.7909E-5T_f{}^3 - 4.6343E-8T_f{}^4 \tag{23}$$

$$c_{pf} = 27089 - 234.67T_f + 0.8971T_f{}^2 - 0.0015242T_f{}^3 + 9.7841E-7T_f{}^4 \tag{24}$$

$$k_f = 0.70611 - 0.0054621T_f + 3.2801E-5T_f{}^2 - 6.3266E-8T_f{}^3 + 3.7935E-11T_f{}^4 \tag{25}$$

$$\mu_f = \frac{4.5E13T_f{}^{-5.7342}}{T_f}$$

Air (valid between 144 and 588 K)

$$\rho_f = 6.1386 - 0.039529T_f + 0.00011942T_f{}^2 - 1.7085E-7T_f{}^3 + 9.3283E-11T_f{}^4 \tag{27}$$

$$c_{pf} = 971.64 + 0.41312T_f - 0.0020033T_f{}^2 + 4.1345E-6T_f{}^3 - 2.6307E-9T_f{}^4 \tag{28}$$

$$k_f = -0.0059297 + 0.00016622T_f - 2.3285E-7T_f{}^2 + 1.6816E-10T_f{}^3 \tag{29}$$

$$\mu_f = -2.4117E-6 + 1.1108E-7T_f - 1.6965E-10T_f{}^2 + 1.2545E-13T_f{}^3 \tag{30}$$

Hydrogen (valid between 33 and 588 K)

$$\begin{aligned}\rho_f &= 1.1291 - 0.014978T_f + 8.692E-5T_f{}^2 - 2.4886E-7T_f{}^3 \\ &+ 3.4488E-10T_f{}^4 - 1.8446E-13T_f{}^5\end{aligned} \tag{31}$$

$$c_{pf} = 9260.7 + 31.544T_f - 0.061696T_f{}^2 + 3.9398E-5T_f{}^3 \tag{32}$$

$$k_f = 0.00024884 + 0.000739T_f - 5.7022E-7T_f{}^2 + 3.62E-10T_f{}^3 \tag{33}$$

$$\mu_f = 3.9331E-7 + 4.3133E-8T_f - 5.9384E-11T_f{}^2 + 4.3768E-14T_f{}^3 \tag{34}$$

Oxygen (valid between 260 and 500 K)

$$\rho_f = 2.4388 - 0.0048859T_f + 4.4665E-6{T_f}^2 \tag{35}$$

$$c_{pf} = 493.9 + 4.5141T_f - 0.017837{T_f}^2 + 3.0909E-5{T_f}^3 - 1.9617E-8{T_f}^4 \tag{36}$$

$$k_f = 0.0089832 + 7.2503E-5T_f - 5.8431E-8{T_f}^2 \tag{37}$$

$$\mu_f = -0.0001765 + 2.0394E-6T_f - 7.855E-9{T_f}^2 + 1.3291E-11{T_f}^3 - 8.2809E-15{T_f}^4 \tag{38}$$

Cooling Flow Over a Single Plate

The average heat transfer coefficient ($\overline{h}$), given in equation (39), is based on the length of the plate in the direction the fluid is flowing (w), the average Nusselt number ($\overline{N}_u$) over the plate and the thermal conductivity of the cooling fluid (k_f).

$$\overline{h} = \frac{\overline{N}_u k_f}{w} \tag{39}$$

The calculation of the average Nusselt number is dependent on whether the flow is laminar over the entire plate or whether it transactions to turbulent flow at some point along the plate. For laminar flow, the average Nusselt number is given by equation (40). For flow that transitions to turbulent at some point along the length of the plate, it is given by equation (41) (ref. 1). These equations are based on the Reynolds number (R_e) and the Prandtl (P_r) number for the fluid flow over the plate.

$$\overline{N}_u = 0.664 R_e^{1/2} P_r^{1/3} \tag{40}$$

$$\overline{N}_u = (0.037 R_e^{4/5} - 871) P_r^{1/3} \tag{41}$$

The Reynolds number and Prandtl numbers are given by equations (42) and (43), respectively. These are based on the cooling flow velocity (V) and the properties of the cooling fluid; density (ρ_f), specific heat (c_{pf}), conductivity (k_f) and dynamic viscosity (μ_f).

$$R_e = \frac{Vw\rho_f}{\mu_f} \tag{42}$$

$$P_r = \frac{c_{pf}\mu_f}{k_f} \tag{43}$$

The Nusselt number, given in equation (40), applies when the Reynolds number over the full plate is less then 5×10^5 whereas equation (41) applies when the Reynolds number exceeds 5×10^5 at some point along the plate, indicating turbulent flow. The Prandtl number range for both equations is between 0.6 and 50 (ref. 1).

Using equations (39) to (43) the average convective coefficient for the cooling fluid over a single plate can be determined. Using the curve fits for the properties of the different fluids, convective coefficients were determined over a range of flow rates and at different operational temperatures. These are shown in figures 15 and 16 for water and the selected gasses, respectively.

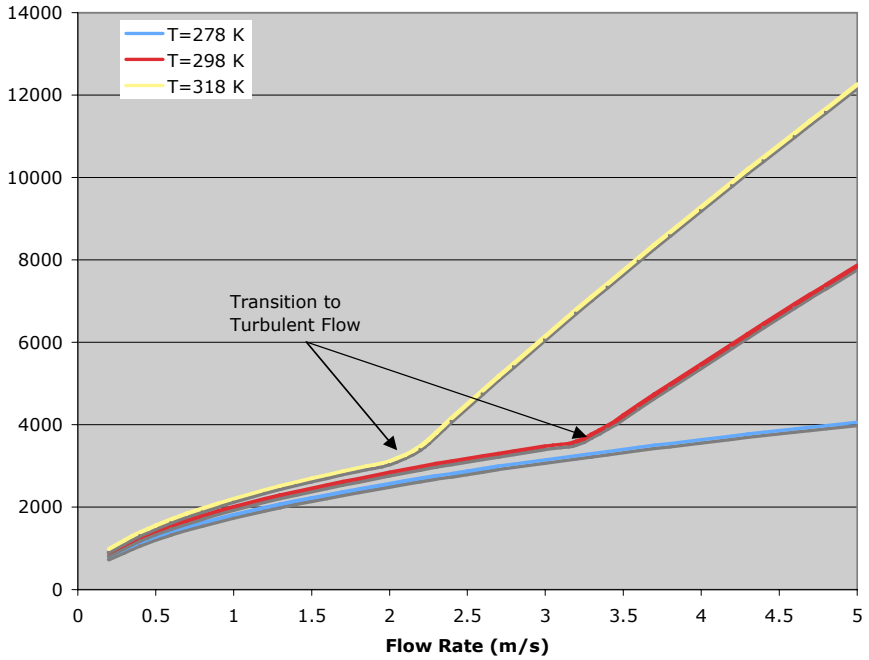

Figure 15.—Convection coefficient as a function of flow rate for water over a single cooling plate.

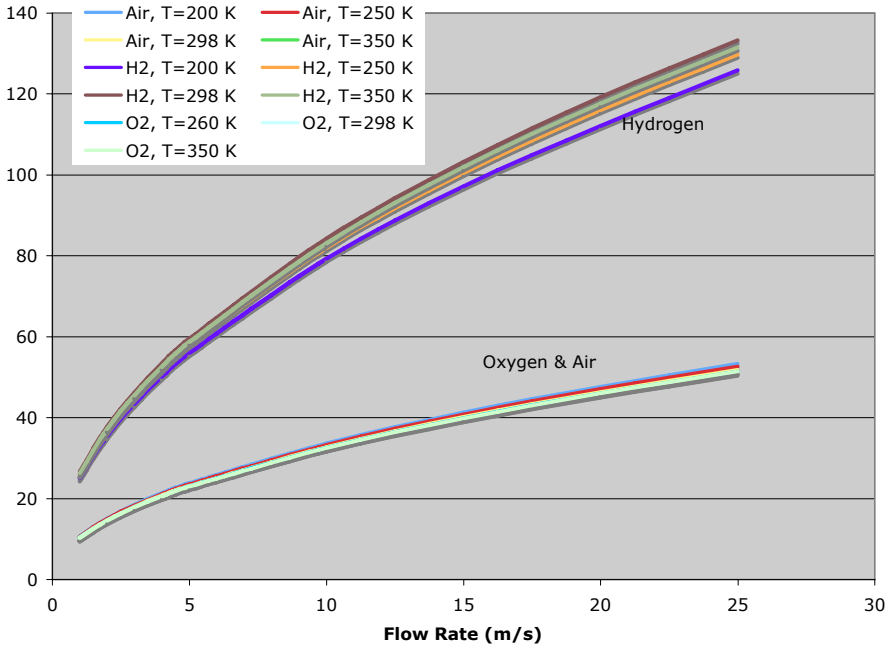

Figure 16.—Convection coefficient as a function of flow rate for hydrogen, oxygen and air over a single cooling plate.

The convective coefficient for water, as shown in figure 15, is fairly dependent on the operating temperature of the water. As can be seen in this figure the higher the water, temperature the greater the convective coefficient. This is due mainly to the fact that at higher temperatures the water will transition to turbulent flow at lower flow rates. At the lowest temperature examined, 278 K, the flow remained laminar over the complete flow rate range. However at higher temperatures the flow transitions to turbulent within this range thereby inducing an increase in the convective heat transfer coefficient. This transition occurs at approximately 3.4 m/s for water at a temperature of 298 K and 2.1 m/s for water at a temperature of 318 K. From this it can be deduced that increasing the operational temperature of the cooling water can provide a benefit by inducing transition to turbulent flow and thereby increasing the convective heat transfer coefficient. However, the increased water temperature will also reduce the temperature difference between the plate and the cooling fluid thereby reducing the heat transfer to the fluid. For a given flow rate, there will be a tradeoff between the convective coefficient and temperature difference between the fluid and the plate that will need to be considered in order to select the optimum flow rate and coolant temperature.

The convective coefficients for the gases that were considered, shown in figure 16, are much less than those for water, as should be expected. These coefficients were generated based on the gas at 1 atm pressure. Of the gases examined, Hydrogen provided the greatest convection capability. The convective coefficient for Hydrogen varied somewhat with temperature over the range of flow rates. The difference increased as the flow rate increased. The convective coefficient was highest for the mid temperature level of 298 K and decreased at both higher and lower temperatures. Oxygen and Air produced very similar convection coefficients over the flow rate range with a much smaller dependence on operational temperature compared to hydrogen.

Cooling Flow Between Parallel Plates

As with the single plate, an analysis to determine the convective heat transfer coefficient between closely spaced parallel plates was also performed. The calculation of the convective coefficient is similar to that for a single plate but utilizes hydraulic diameter (d_h) instead of the length of the plate in the analysis. Equation (44) is the convective coefficient for flow between parallel plates. The hydraulic diameter, given by equation (45), is based on the cross-sectional area through which the fluid flows and the wetted perimeter. These quantities are based on the plate length perpendicular to the flow (L) and the plate spacing (d).

$$\overline{h} = \frac{\overline{N}_u k_f}{d_h} \tag{44}$$

$$d_h = \frac{4Ld}{(2L + d)} \tag{45}$$

The flow between the plates is considered laminar if the Reynolds number of the flow is below 2,300. The Reynolds number for flow between the plates is given by equation (46). The Reynolds number is based on the spacing between the plates instead of the plate length as it is for the single plate analysis.

$$R_e = \frac{Vd\rho_f}{\mu_f} \tag{46}$$

For laminar flow between the plates the Nusselt number is given by equation (47). This equation represents a curve fit to empirical data (ref. 1) on the relationship between Nusselt number and the ratio of the plate spacing to the plate length perpendicular to the fluid flow. This equation is valid for L/d ratios of less then 65. For L/d ratios above 65 the Nusselt number is a constant with a value of 8.23.

$$\overline{N}_u = 1.5137 \ln\left(\frac{L}{0.11848d} + 1\right) - 0.020265\frac{L}{d} \tag{47}$$

For Reynolds numbers greater then 2300 it is assumed that the flow within the passage between the plates is turbulent. For this condition the Nusselt number is given by equation (48), which is based on the Prandtl number, given by equation (43) and the friction factor (f) for the surface of the plates. For a smooth surface, the friction factor can be estimated by equation (49) (ref. 1). This Nusselt number equation for turbulent flow between the plates is valid for Reynolds numbers between 2,300 and 5×10^6 and for Prandlt numbers between 0.5 and 2,000.

$$\overline{N}_u = \frac{(f/8)(R_e - 1000)P_r}{1 + 12.7(f/8)^{1/2}(P_r^{2/3} - 1)} \tag{48}$$

$$f = (0.79 \ln R_e - 1.64)^{-2} \tag{49}$$

Using the above analysis, results were generated for the various cooling fluids (water, air, hydrogen and oxygen). The results for water are shown in figure 17. At the smaller plate spacing the Reynolds number is low enough that the flow is initially laminar at low flow rates. This can be seen on the curves for the plate spacing of 0.25 to 1.0 cm. This initial laminar flow produces a nearly level convective coefficient with increasing flow rate. Once the flow rate reaches the level in which transition to turbulent flow occurs, the convective coefficient begins to increase with increasing flow rate. The transition to turbulent flow occurs at lower flow rates with the parallel plates than in the single plate analysis. This produces a larger convective coefficient for all of the plate spacings examined over the single plate analysis. For water the larger plate spacing generally produced a greater convective coefficient at a given flow rate. Therefore with water as the cooling fluid, there is not only a mass benefit but also a heat transfer benefit in utilizing less cooling plates and having them spaced further apart.

The convective coefficients for the gasses, air, oxygen and hydrogen are shown in figures 18 to 20, respectively. As with the water results, the convective coefficients are fairly steady under laminar flow conditions. Once transition to turbulent flow occurs, there is a general increase in the convective coefficient with flow rate. As with the single plate analysis, Hydrogen produces the highest convective coefficients of the gases examined. Unlike the water analysis, for the gasses in general, the closer the plate spacing the greater the heat transfer coefficient. Therefore to optimize the heat transfer with a gas as the cooling fluid, the greatest number of plates should be utilized.

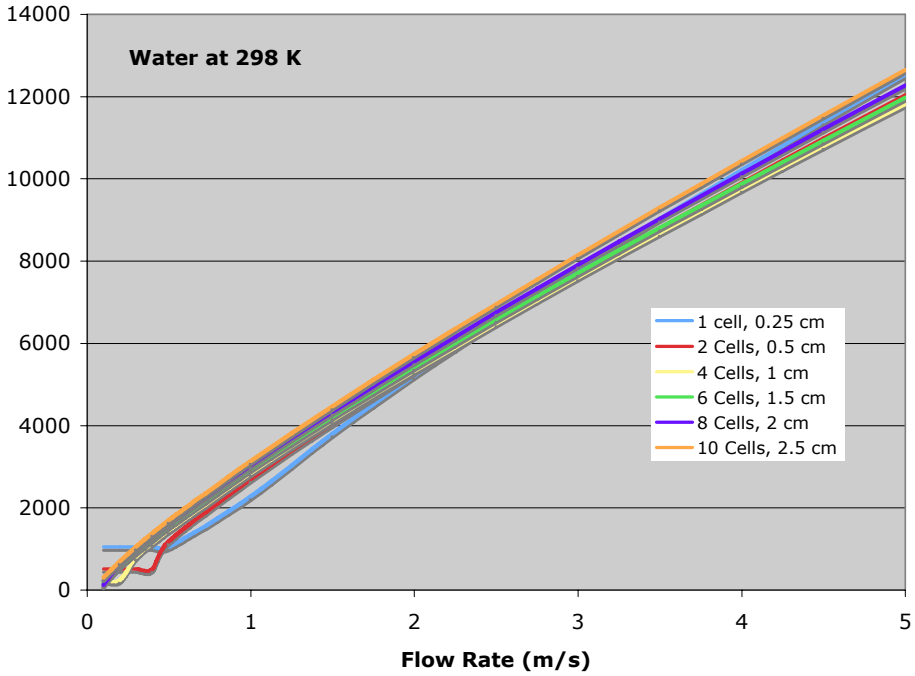

Figure 17.—Convective coefficient for water versus flow rate for various plate spacing.

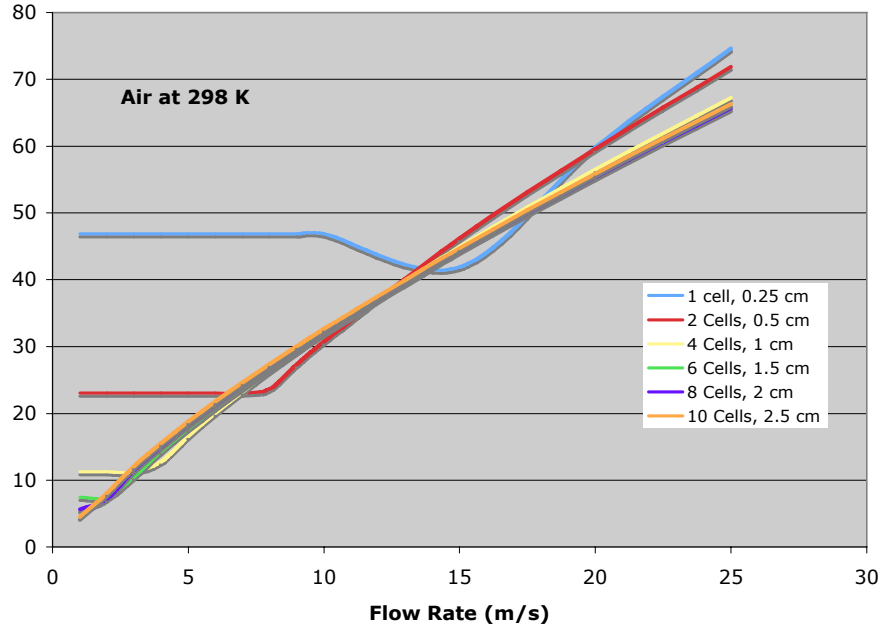

Figure 18.—Convective coefficient for air versus flow rate for various plate spacing.

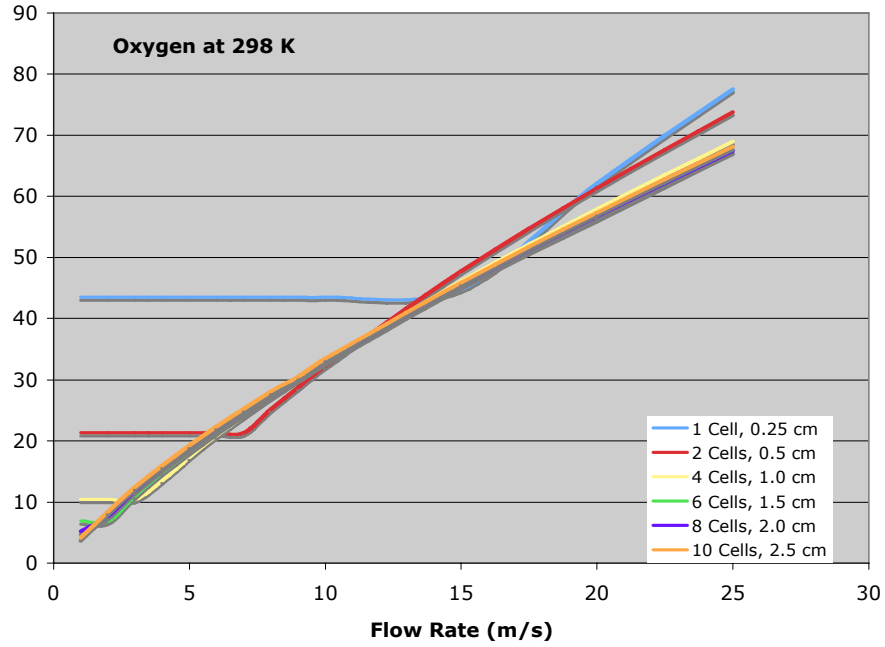

Figure 19.—Convective coefficient for oxygen versus flow rate for various plate spacing.

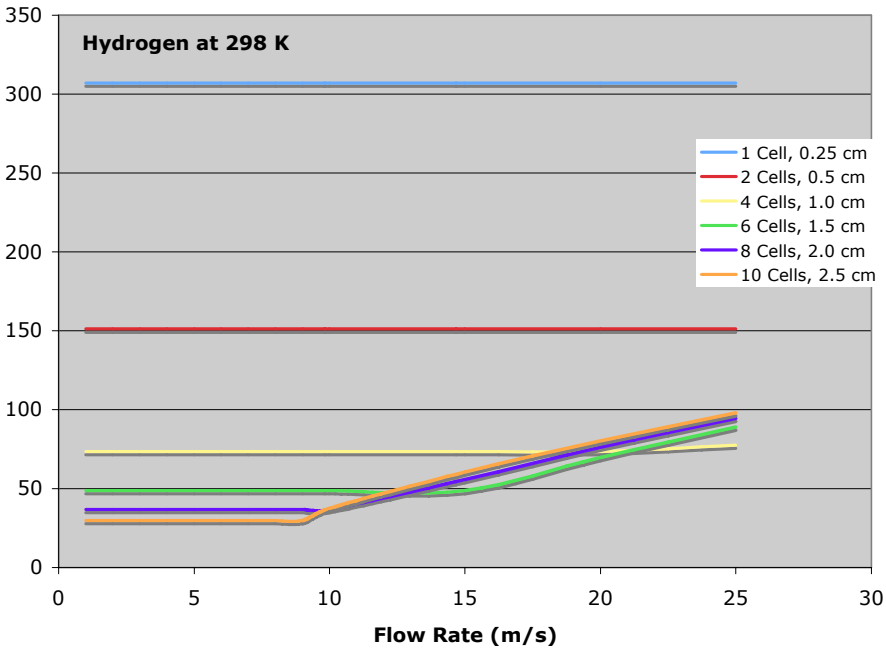

Figure 20.—Convective coefficient for hydrogen versus flow rate for various plate spacing.

Temperature Distribution Analysis

If a single cooling plate is utilized to remove heat from a number of the cells then the actual cell temperature will vary between the cells closest to the cooling plate and the ones further away. The variation in cell temperature will depend on the thermal conductivity of the cell and the contact resistance between the cells. Due to the thinness of the MEA it is assumed that the MEA will be at a uniform temperature. The heat transfer path between the cells is illustrated in figure 21.

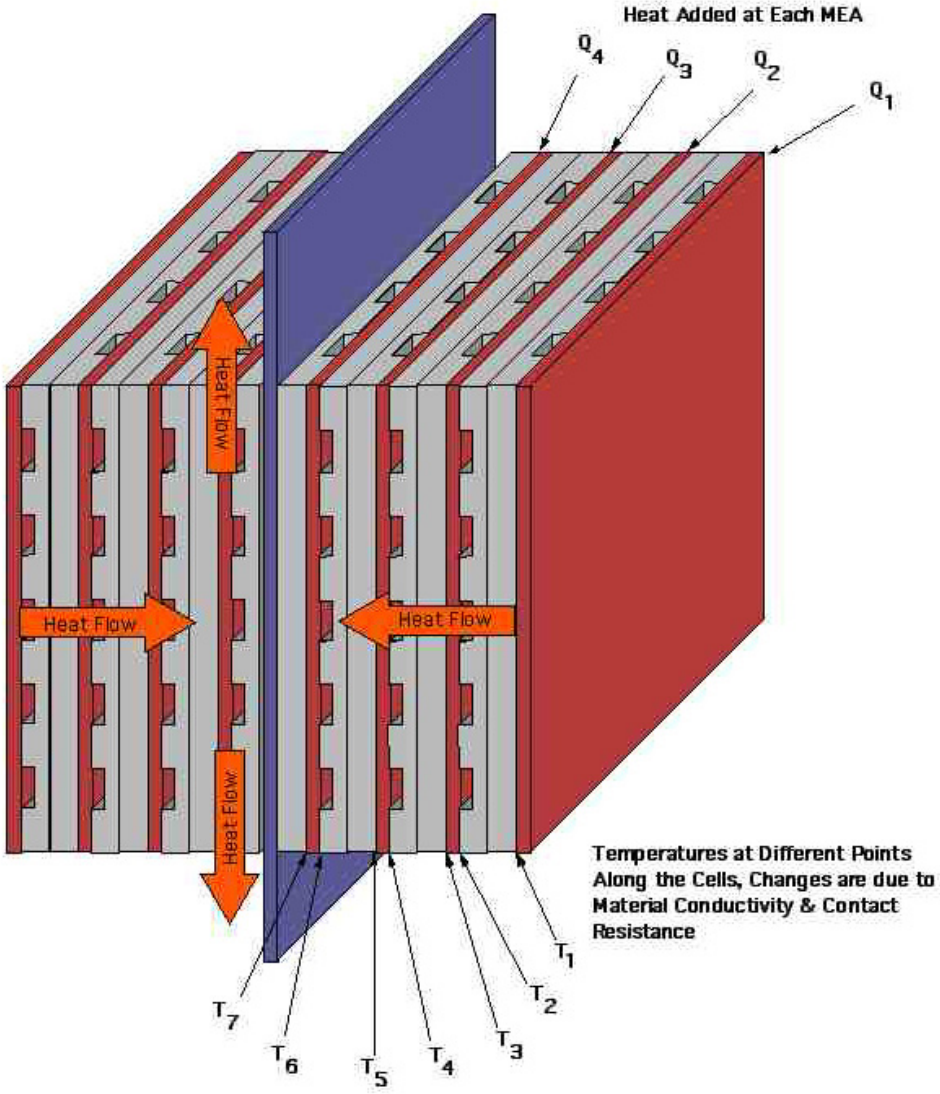

Figure 21.—Heat transfer from multiple cells to the cooling plate.

As shown in figure 21, the heat from each cell will flow toward the cooling plate. It should be noted that this heat will enter the cooling plate from both sides. Therefore, for a given number of cells per cooling plate, half of them will be on one side of the cooling plate and the rest on the other side. There will be temperature changes across the bipolar plates as well as across the interfaces between the cells due to the conductivity of the bipolar plates (k_c) and the contact resistance (R) between them. Because of its thinness and its being the source of the heat produced, the thermal resistance across the MEA was not considered in this analysis. Similarly, because the MEA is a flexible membrane and will deform providing good contact between the MEA and the bipolar plate, the contact resistance between the bipolar plate and MEA was assumed to be minimal and not considered in order to simplify the analysis. The conductivity for a graphite plate is given in table 1. The contact resistance between the bipolar plates of adjacent cells was assumed to be 9×10^{-5} m^2K/W (ref. 2). This contact resistance is representative of the contact between two smooth flat surfaced being pressed together. Various approaches can be used to decrease this contact resistance such as increasing the contact pressure or utilizing a highly conductive thermal coating or filler (such as indium foil) between the plates. These approaches could produce an order of magnitude reduction in the contact resistance.

The maximum cell temperature, which would occur at the cell furthest from the cooling plate (T_1), is represented by equations (50) and (51) for an even and odd number of cells per cooling plate respectively. These equations are based on the heat flow produced by each cell (Q_c), the number of cells per cooling plate (n), the cell area (A_c), thickness (t_c) and the desired temperature of the cooling plate (T_o).

$$T_1 = \left(\frac{2n + n^2}{8}\right)\left(\frac{RQ_c}{A_c} + \frac{Q_c t_c}{k_c A_c}\right) + T_o \tag{50}$$

$$T_1 = \frac{1}{8}\left(\frac{RQ_c}{A_c} - \frac{3Q_c t_c}{k_c A_c}\right) + \left(\frac{2n + n^2}{8}\right)\left(\frac{RQ_c}{A_c} + \frac{Q_c t_c}{k_c A_c}\right) + T_o \tag{51}$$

From the above equations, the difference between the maximum cell temperature and the cooling plate temperature can be determined. This is plotted in figure 22 as a function of the number of cells, which transfer heat to a single cooling plate. The higher the cell number the further apart the cooling plates would be placed within the stack. Also plotted in figure 22 is a representative required cooling plate thickness. This cooling plate thickness is for a plate with a conductivity of 800 W/m K and water as the cooling fluid. The change in the cooling plate thickness with the increase in the number of cells is due to the added heat being transferred to the cooling plate with each additional cell, as well as the slightly reduced cooling plate operational temperature due to the requirement of maintaining the hottest cell at a temperature of 352 K or less.

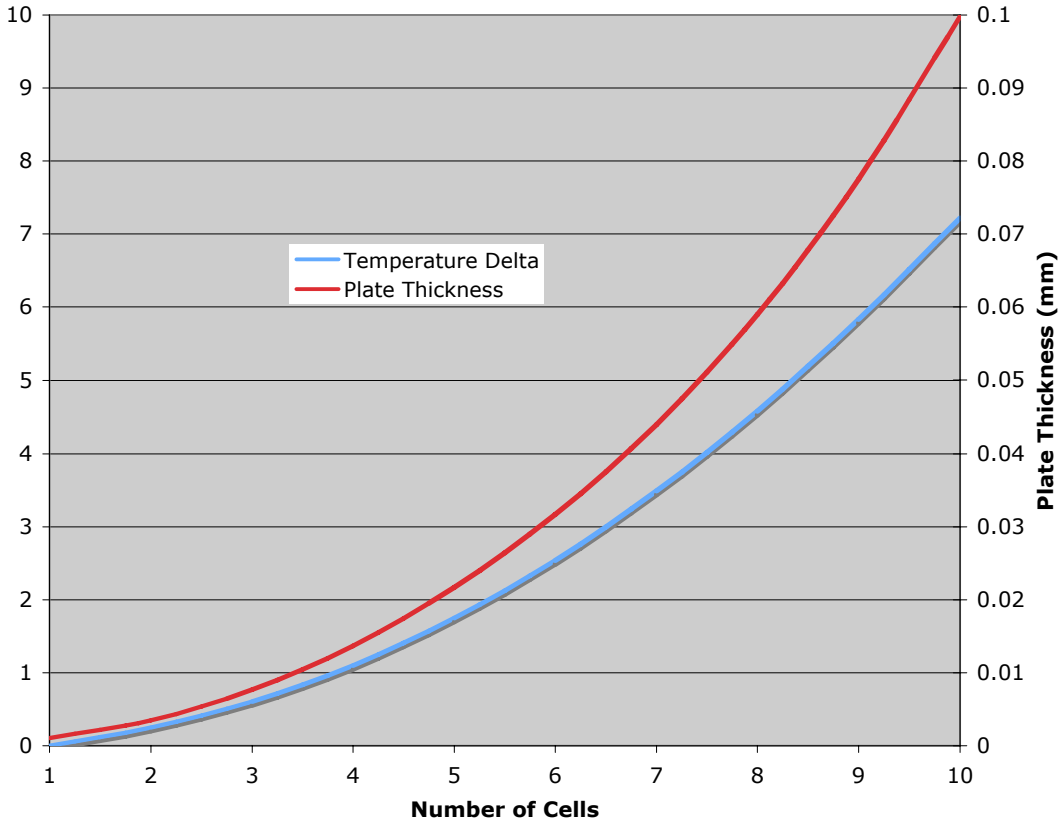

Figure 22.—Temperature change between cooling plate and furthest cell.

From figure 22 it can be seen that the change in temperature between the cooling plate and the cell furthest from it increase exponentially as the number of cells transferring heat to the cooling plate increases. The temperature of the cell furthest from the cooling plate represents the maximum cell temperature within the stack. Therefore figure 22 indicates what the cooling plate temperature will need to be in order to maintain all of the cells below this maximum temperature. For example, if there are 10 cells on a side transferring heat to one cooling plate with a maximum allowable cell temperature of 353 K, the cooling plate temperature would need to be approximately 347 K to insure all cells are below the maximum allowable temperature. As shown in the previous section, reducing the cooling plate temperature will reduce the heat transfer to the cooling fluid requiring either a corresponding reduction in the cooling fluid temperature or an increase in the cooling plate thickness and/or area. This result however, does show that this required temperature reduction of the cooling plate is relatively small especially for the lower range of the number of cells transferring heat to the cooling plate. From this it would indicate that there would be little disadvantage to using one cooling plate for multiple cells. This would reduce the number of cooling plates required, reducing the stack weight, volume and complexity.

The next step in evaluating the heat flow within the cells of the stack is to consider the heat flow along the cooling plate and determine the temperature distribution along the cell. This is illustrated in figure 23. The heat generated by the cells is assumed to be produced uniformly over the area of the cell. This heat is then conducted out through the cooling plate and removed from the system. The maximum cell temperature will occur at the center of the cell furthest from where the heat is removed from the plate. To determine this temperature, an equation that models the heat flow from the cells to the plate and then out from the stack must be derived. To simplify the analysis, it is assumed that no heat is lost along the

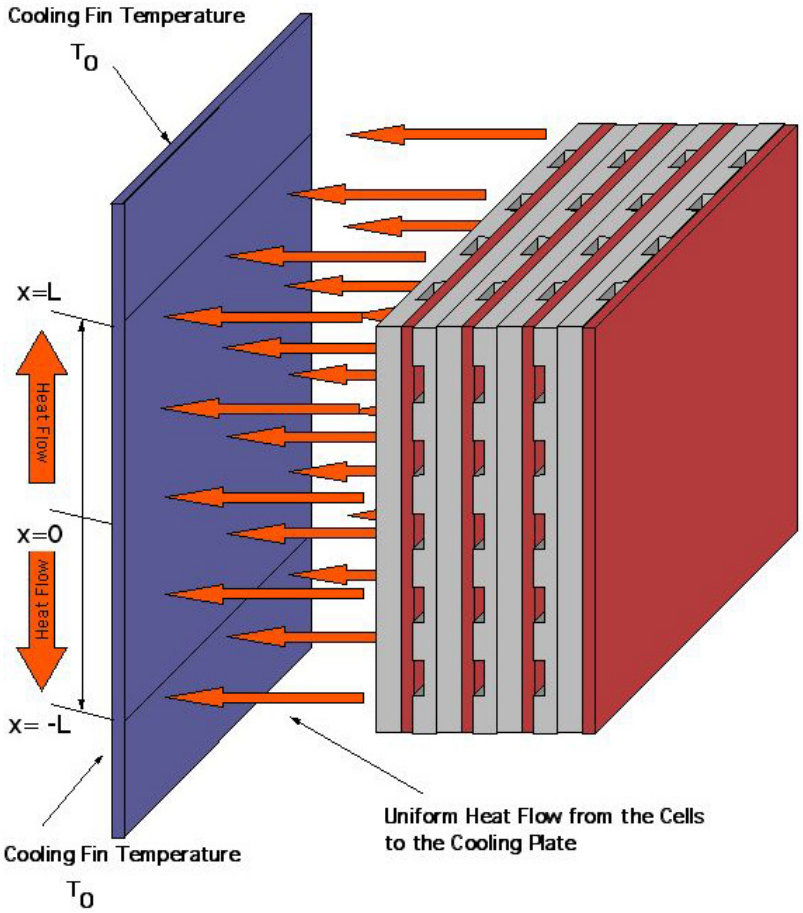

Figure 23.—Heat transfer from the stack cells to the cooling plate.

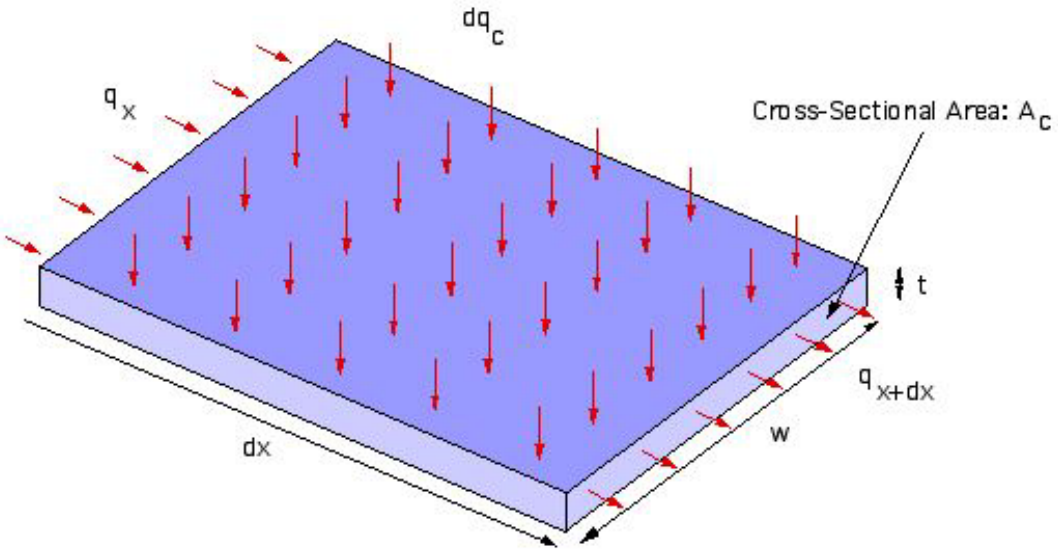

Figure 24.—Cooling plate heat flow diagram.

edges of the stack where the cooling plate is even with the stack cells. All of the heat is conducted to and removed from the portion of the cooling plate that extends beyond the stack cells. This is a conservative assumption since any additional heat transfer from the stack, other then from the extended plates, will reduce the heat that flows to the cooling plates.

Utilizing the coordinate system shown in figure 23, the maximum cell and plate temperature will occur at the center of the plate, the location $x = 0$. To determine this maximum temperature on the cooling plate, an energy balance is used to equate the heat flow into the plate and out through the portions of the plate extended beyond the stack.

For an incremental segment of the cooling plate the heat flow in (q_x) plus the addition of heat flow from the cells (dq_c) is equal to the heat flow out (q_{x+dx}) as given by equation (52) and illustrated in figure 24.

$$q_x + dq_c = q_{x+dx} \tag{52}$$

Expressions for each term in equation (51) can be substituted (shown in equation (53)) yielding the differential equation for the heat transfer along the plate, given by equation (54).

$$kA_c \frac{dT}{dx} + nq_c w dx = kA_c \frac{dT}{dx} + kA_c \frac{d^2T}{dx^2} dx \tag{53}$$

$$\frac{d^2T}{dx^2} + \frac{nq_c w}{kA_c} = 0 \tag{54}$$

The differential equation, given by equation (54), is solved by integrating and utilizing the boundary conditions of $T = T_0$ at $x = L$ and $T = T_0$ at $x = -L$. This results in the following expression for the temperature along the cooling plate.

$$T = \frac{nq_c w}{2kA_c}(L^2 - x^2) + T_0 \tag{55}$$

The heat flow per area from each cell (q_c), is multiplied by the total number of cells being cooled by each cooling plate (n) to determine the total heat flow into the cooling plate. Calculating the maximum plate temperature and increasing this by the ΔT given in figure 22 for the corresponding number of cells on each side of the cooling plate (n_s) determines the maximum cell temperature. For example, if four adjacent cells are transferring heat to one side of the cooling plate and the maximum temperature of the cooling plate is calculated to be 350 K, from equation (55), then the maximum cell temperature will be 351 K based on the 1 K increase in temperature across four cells given by figure 22. A regression was performed on this relationship between the number of cells and the rise in temperature across them (ΔT). This relationship is given by equation (56).

$$\Delta T = -0.045133 - 0.0079181 n_s + 0.073379 {n_s}^2 \tag{56}$$

Results and Conclusions

The analysis described in the previous section provides a means of modeling the heat flow from the individual cells to a cooling plate and then out to the external cooling fluid. Through this analysis the required plate thickness needed to maintain the fuel cell stack at a desired temperate can be determined for various types of plate materials. Utilizing the baseline operating temperature specified in table 3 (353 K), results were generated to determine the required cooling plate thickness for various plate conductivities and over a range of cells per cooling plate. These results are shown in figures 25 to 28 for the various cooling fluids. The plate thickness is determined through an iterative process between the heat extracted by the cooling fluid, equation (21), and the heat transported from the cells to the plate and the corresponding plate temperature just outside the fuel cell stack (T_0), equation (55). This plate temperature at the boundary of the fuel cell stack is also plotted on these figures. The analysis also includes the variation in convective coefficient, given by equation (44), due to the difference in plate spacing for the range of cells per cooling plate examined.

The analysis was applied to the baseline fuel cell stack given in table 3. Figure 25 shows the required plate thickness with water as the cooling fluid. The water flow rate was set a 1 m/s which produced a convective coefficient of between 2,711 and 3149 W/m^{2}K, as shown in figure 17, over the range of cells per cooling plate examined. From this figure it can be seen that the plate thickness were fairly small. A plate thickness of 1 mm is considered the upper limit of what is desirable for the cooling plates. Even at the lower plate conductivities, the plate thickness is at a millimeter or less over the majority of the range of cells per cooling plate examined. This indicates that with water as the cooling fluid there are a number of potential plate cooling materials that can be utilized to provide a compact effective cooling system for the fuel cell. Also there were significant benefits seen in reducing the cooling plate thickness with increasing cooling plate thermal conductivity. With water as the cooling fluid, a high conductivity cooling plate can be utilized to cool multiple cells of the fuel cell stack. This could provide a reduction in the complexity, volume and mass of the fuel cell stack. Figures 26, 27, and 28 show the required plate thickness and plate temperature at the boundary of the stack for air, oxygen and hydrogen as the cooling fluid, respectively. For these gasses a flow rate of 15 m/s was utilized for each.

For air as the cooling fluid, shown in Figure 26, the required plate thicknesses are very large for most of cells per cooling plate examined. To achieve a cooling plate thickness on the order of 1 mm would require the use of a single cooling plate for every one to two cells. There was also no benefit seen by increasing the conductivity of the cooling plate over the complete range of cells per cooling plate. This is due to the lower convective coefficient of air, which was in the range of between 42 and 46 W/m^{2}K, compared to that of water.

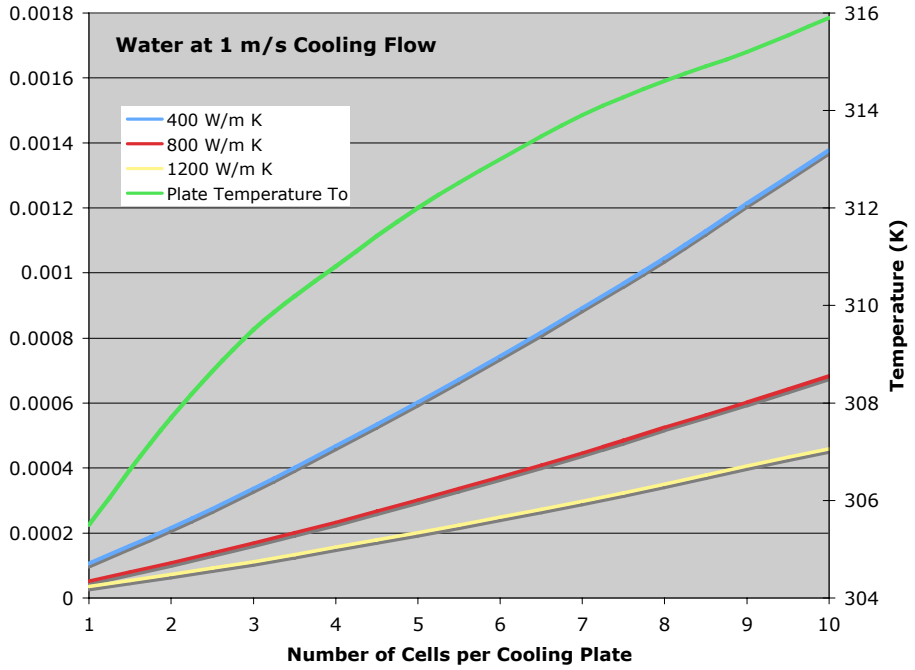

Figure 25.—Required cooling plate thickness for maximum internal temperature of 353 K with water as the cooling fluid.

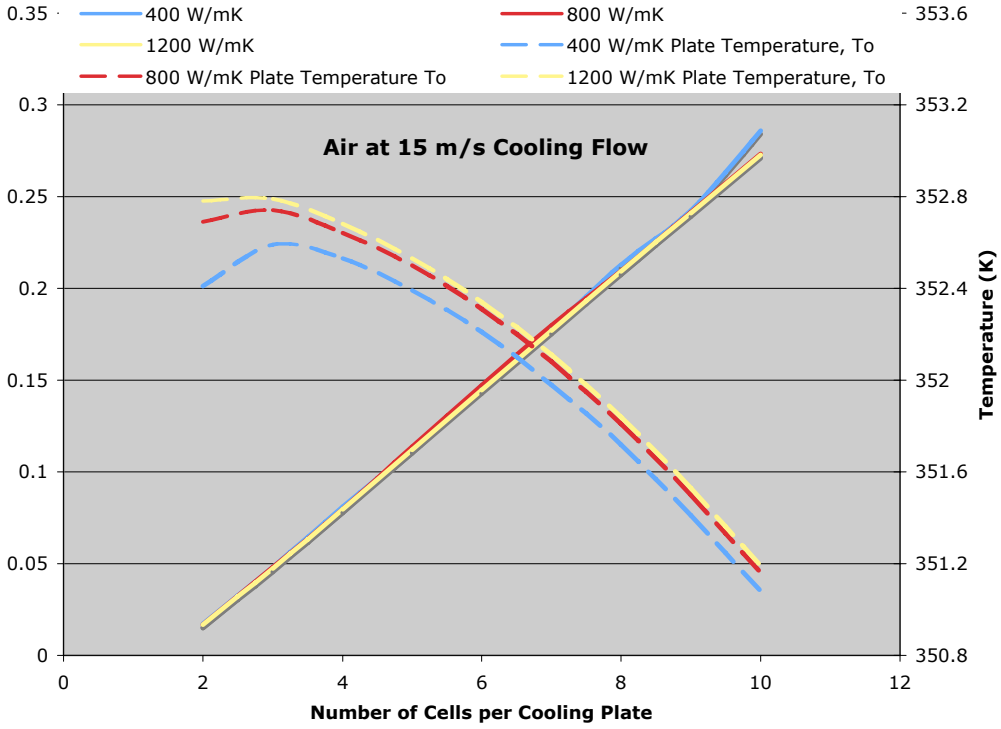

Figure 26.—Required cooling plate thickness for maximum internal temperature of 353 K with air as the cooling fluid.

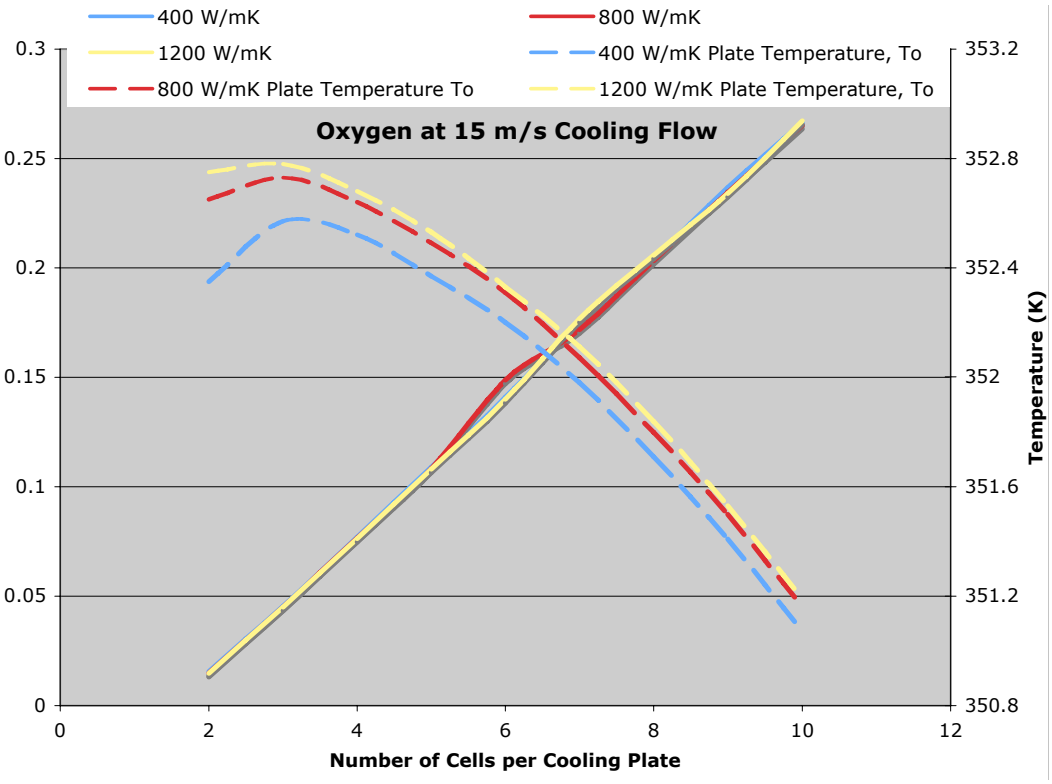

Figure 27.—Required cooling plate thickness for maximum internal temperature of 353 K with oxygen as the cooling fluid.

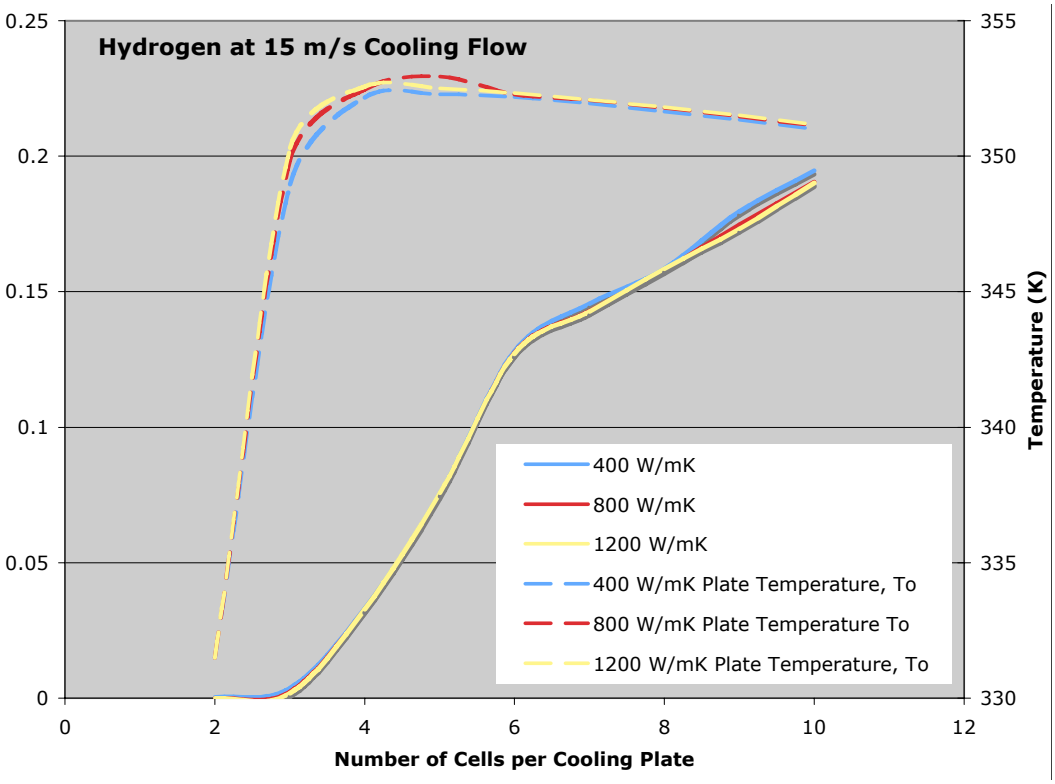

Figure 28.—Required cooling plate thickness for maximum internal temperature of 353 K with hydrogen as the cooling fluid.

The results for cooling plate thickness with oxygen as the cooling fluid, shown in figure 27, are very similar to those with air as the cooling fluid. This should be expected since the convective coefficients of both these gasses are very similar over the range of plate spacing, as shown by figures 18 and 19. The convective coefficient of oxygen for the plate spacing corresponding to the cells per cooling plate, given in figure 27, is between 43 and 48 W/m^2K. As with air, the plate conductivity did not have a significant effect on the cooling plate size. And a cooling plate would need to be utilized for each one or two cells in order to achieve a reasonable cooling plate thickness.

The last cooling gas considered, hydrogen, has a much larger range of convective coefficients over the corresponding cooling plate spacing associated with the range of cells per cooling plate utilized. This range of convective coefficient was between 50 and 303 W/m^2K. This larger range of convective coefficient enabled small cooling plate thickness for up to 3 cells per cooling plate. As with the other gases there was little effect of increasing thermal conductivity of the plate on the required thickness, except in the range of three cells per cooling plate and less. This trend is not evident in figure 28 due to the graph scale, therefore this region has been plotted in figure 29 to show this effect of conductivity on the required plate thickness for 1 and 2 cells per cooling plate.

For a lower number of cells per cooling plate, one or two cells per plate, the required cooling plate thickness with gaseous hydrogen, as the cooling fluid, is fairly small within the few millimeter range. Also there is an appreciable benefit in reducing the required thickness with an increase in the plate conductivity, as can be seen in figure 29. However, beyond one or two cells per plate the required cooling plate thickness becomes too large to be practically applied to the fuel cell. To utilize any of the examined gasses as a cooling fluid will require a cooling plate for each cell or possibly two cells at best.

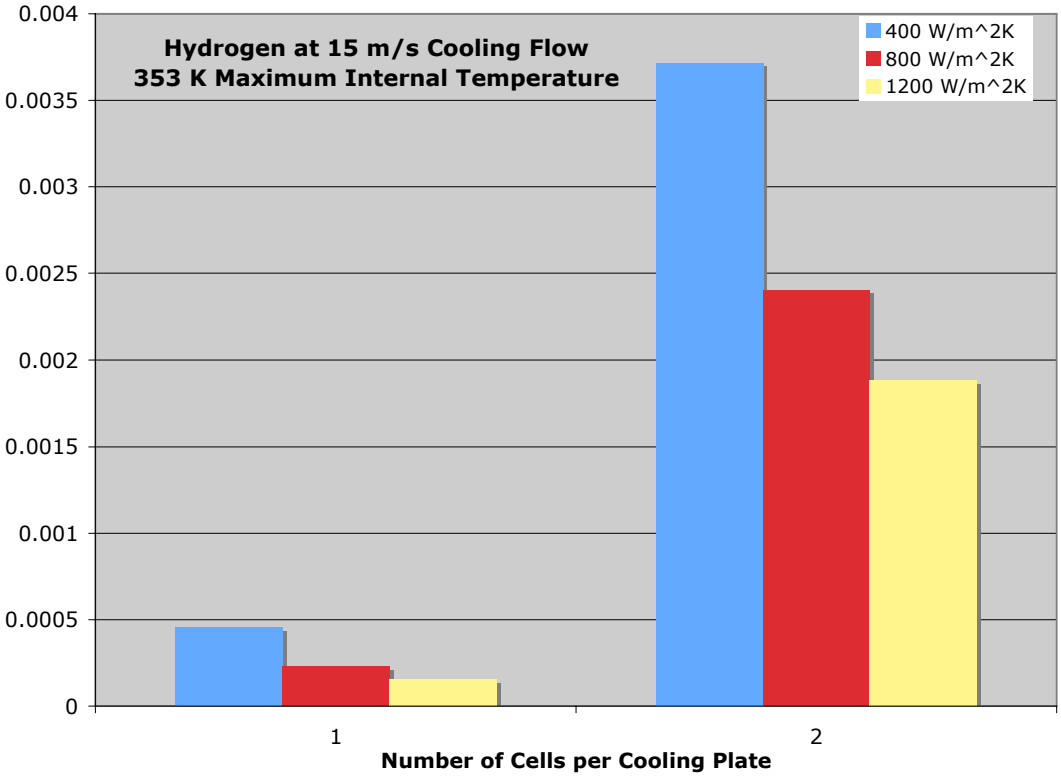

Figure 29.—Required Cooling plate thickness with hydrogen as the cooling fluid for small cell per cooling plate values.

The results shown in figures 25 to 29 indicate that to minimize the number of cooling plates requires a cooling fluid with a high convective coefficient, such as water. The cooling plate thermal conductivity, over the range examined, was only a factor if the convective coefficient was order of a few hundred W/m^2K or greater. For convective coefficients below this there was little benefit to utilizing a high conductivity cooling plate.

The benefits of water as the cooling fluid, such as reduced cooling plate thicknesses and the ability to cool multiple cells with a single cooling plate, were illustrated in figure 25. However, these results were generated by optimizing the plate operating temperature to minimize the required plate thickness. For a highly convective coefficient fluid, such as water, this produced a significant temperature difference along the cells. This temperature difference is shown in figure 30. This was not the case for the lower conductivity gasses examined. For the gasses the temperature difference across a given cell was minor, on the order of a few degrees at most.

From figure 30, it can be seen that a significant temperature gradient is present across the cells for the water cooled fins. This was the result of optimizing the system to minimize the cooling plate thickness. The temperature profile curves were the same for all conductivities examined due to the optimization on plate thickness. This internal temperature gradient would be detrimental to the operation and life of the cells in the stack. Therefore for high conductivity cooling fluids the plate thickness will need to be optimized to minimize the variation in internal temperature. To achieve this, the cooling plate thickness was sized based on a maximum internal temperature gradient of 3 K. The results of this sizing are shown in figure 31. To achieve this fixed temperature gradient the heat transfer to the fluid has to be adjusted to match the change in cooling plate thickness. This adjustment can be achieved by either changing the flow rate of the cooling fluid and or the coolant flow temperature.

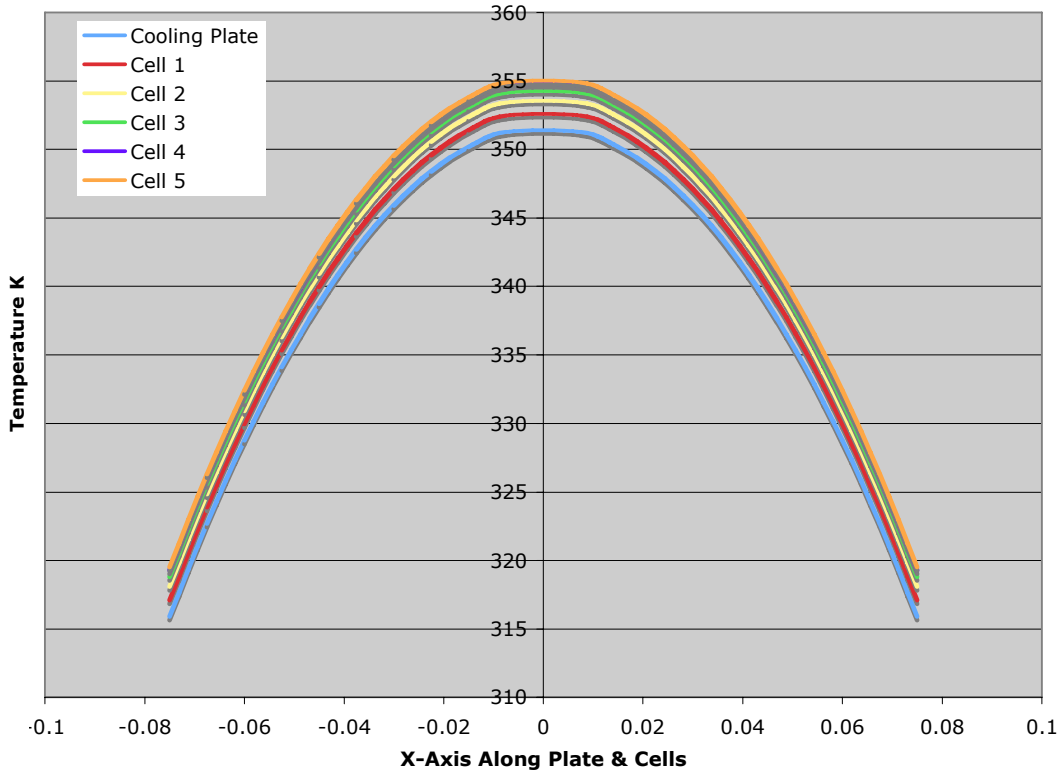

Figure 30.—Temperature profile along each cell for a single cooling plate with heat being removed from both sides (see fig. 21).

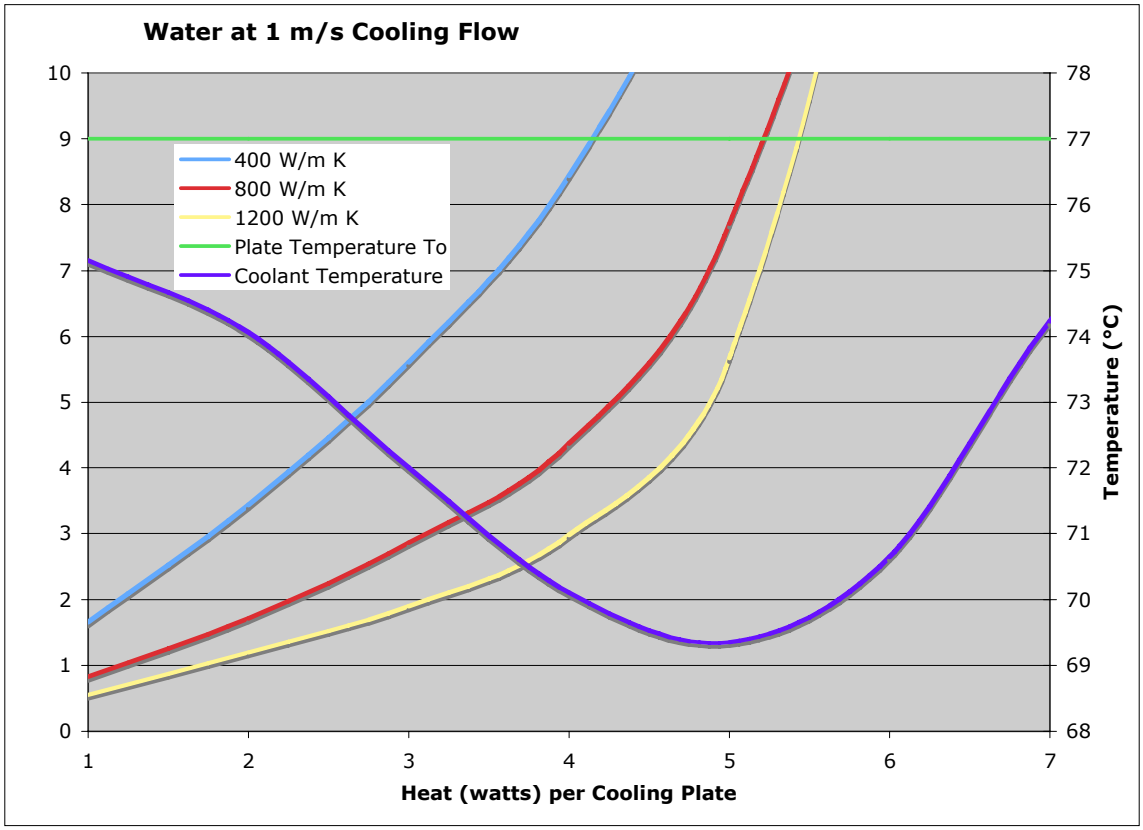

Figure 31.—Required cooling plate thickness for maximum internal temperature of 353 K and maximum gradient of 3 K with water as the cooling fluid.

The number of cells per cooling plate plotted on figure 25 corresponds to the heat load being cooled by each plate. As given in table 3, each cell produced 31.5 W of excess heat. From figure 31 it can be seen that the required plate thickness for the conductivities examined are significantly higher then those shown in figure 25, approximately an order of magnitude larger. The curves in figure 25 were based on minimizing the plate thickness for various plate thermal conductivities over a range of cells per cooling fin. Figure 31 shows the same analysis except that the maximum temperature gradient along any of the cells and from cell to cell was maintained at 3 K. Fixing the temperature gradient required the cooling plate thicknesses to increase to enable greater heat transfer in order to minimize the temperature difference along the cells.

From the results shown in figure 31, it can be seen that there was a significant benefit gained by increasing the thermal conductivity of the cooling plate. Higher conductivities enabled thinner plates to be utilized for a given number of cells per cooling plate or enabled more cells to be cooled by a cooling plate of a given thickness. As the amount of heat removed per cooling plate increases a point is reached where the coolant temperature will begin to rise and the plate thickness increases significantly. This may seem counter intuitive, however it is due to the dual requirement on the cooling plate of being able to remove the desired heat while maintaining a maximum 3° temperature difference within the stack. As the number of cells per cooling plate increases the distance that the heat has to move and corresponding thermal resistance increases. Therefore to maintain the desired temperature gradient the coolant temperature has to be closer to the operating point of the fuel cell. With a fixed coolant flow, the increase in coolant temperature needed to maintain the desired temperature gradient causes the rapid increase in the cooling plate thickness shown in figure 31.

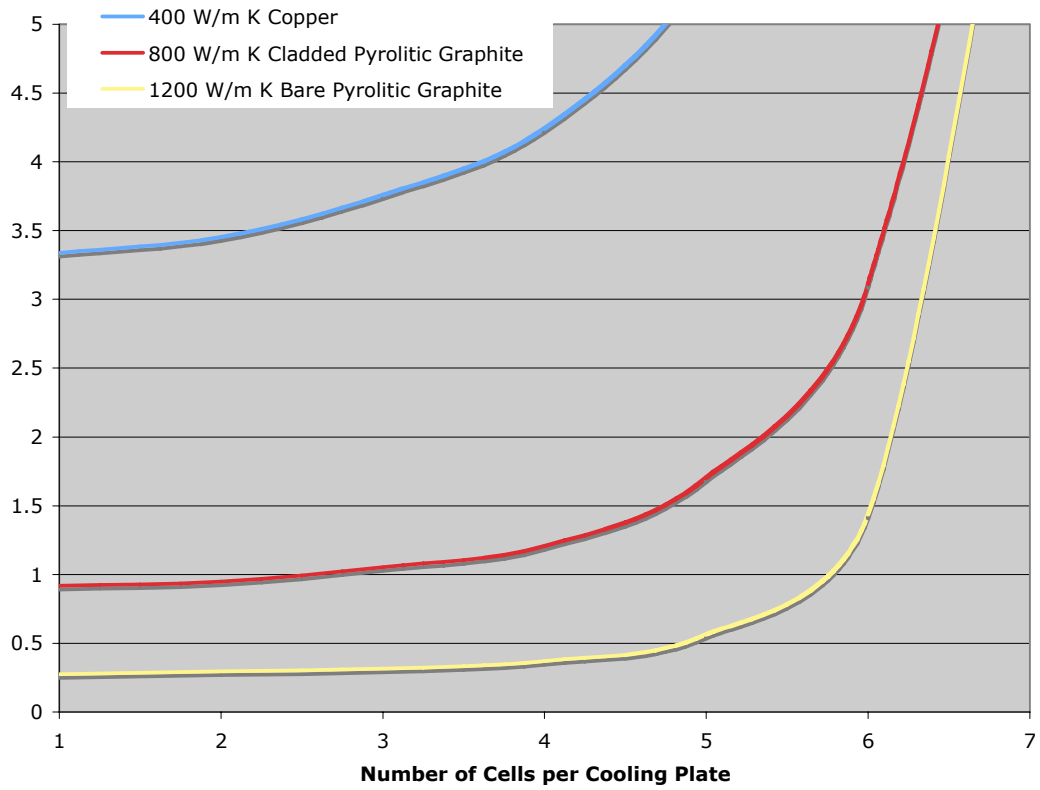

Figure 32.—Total cooling plate mass for a 10 cell stack segment.

The plate thickness, shown in figure 31, can also be a relative measure of the cooling plate mass and how this mass is affected by changing the number of cells per cooling plate. For a fixed cooling plate area, the total cooling plate mass will depend on the number of cooling plates utilized and the thickness of those plates. To illustrate this effect on mass, the total cooling plate mass as a function of the number of cells per cooling plate for a ten-cell segment was plotted in figure 32. The mass of the cooling plates is based on their thickness as determined from the results plotted in figure 31 and material densities corresponding to the various thermal conductivities used, given in table 1. It should be noted that these results were for the case where the maximum temperature gradient within the stack was held to 3 K. From figure 32, it can be seen that the total mass of the cooling plates increases exponentially as the heat load to the plate increases. This is due to the significant increase in required plate thickness, needed to maintain the maximum 3° temperature difference within the stack, as the heat load on the cooling plate increases (number of cells per cooling plate increases).

Another means of determining the effectiveness of the cooling plates is to compare their specific mass in watts of thermal power dissipated per kilogram of total plate mass. This relationship is a gauge of the overall efficiency of the plates with regard to their total mass. These results are shown in figure 33 for various types of cooling plate material. In this figure, the specific cooling capacity (W/kg) of the conductive cooling plates is compared to that of a conventional fluid passage cooling plate.

The conventional plate consists of a 1.2 mm thick graphite plate with an internal cooling fluid channel. An example of this type of cooling plate is shown in figure 34. For this type of plate the estimated cooling capacity was 765 W/kg for the heat load used in this analysis, which is based on the heat load and the plates weight of 85.76 gm. For this analysis it was assumed that the conventional cooling plate would always be capable of removing the applied heat load and maintaining the desired internal temperature distribution. The conductivities and masses of the conductive cooling plates correspond to those used in the previous figures at one cell per cooling plate (copper at 400 W/mK, metal carbon composite at 800 W/mK and the pyrolitic graphite plates at 1200 W/mK). The masses of these

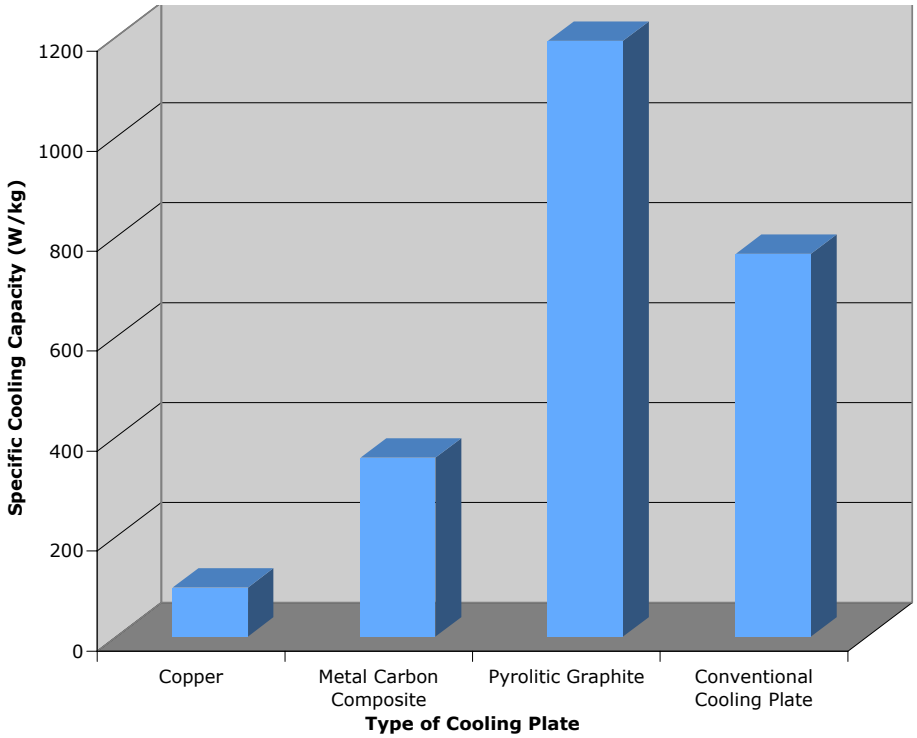

Figure 33.—Comparison of cooling plate specific cooling capacity.

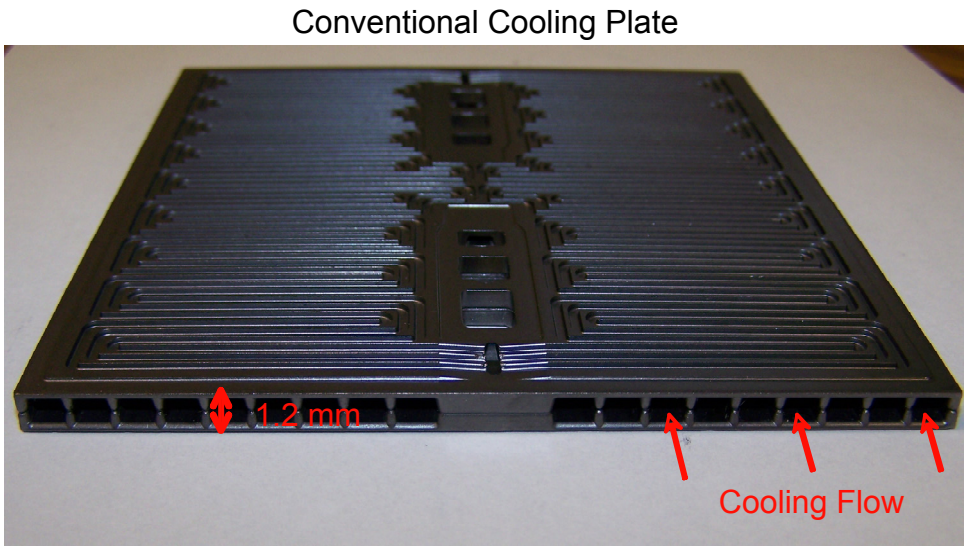

Figure 34.—Example of a conventional cooling plate geometry.

cooling plates, and the heat loads applied, can be translated into a specific cooling capacity figure of merit (thermal watts dissipated per kg of cooling plate), which is displayed for comparison in figure 33. From figure 33, it can be seen that the highest conductivity cooling plate (the bare pyrolitic graphite) provided a greater specific cooling capacity then a conventional internal passage cooling plate. This indicates that improved fuel cell cooling performance can be achieved, over a conventional internal cooling passage system, through the use of high conductivity, lightweight composite cooling plate materials. Specific cooling capacity results were also generated over the range of cells per cooling plate used in figure 32. These results are shown in figure 35.

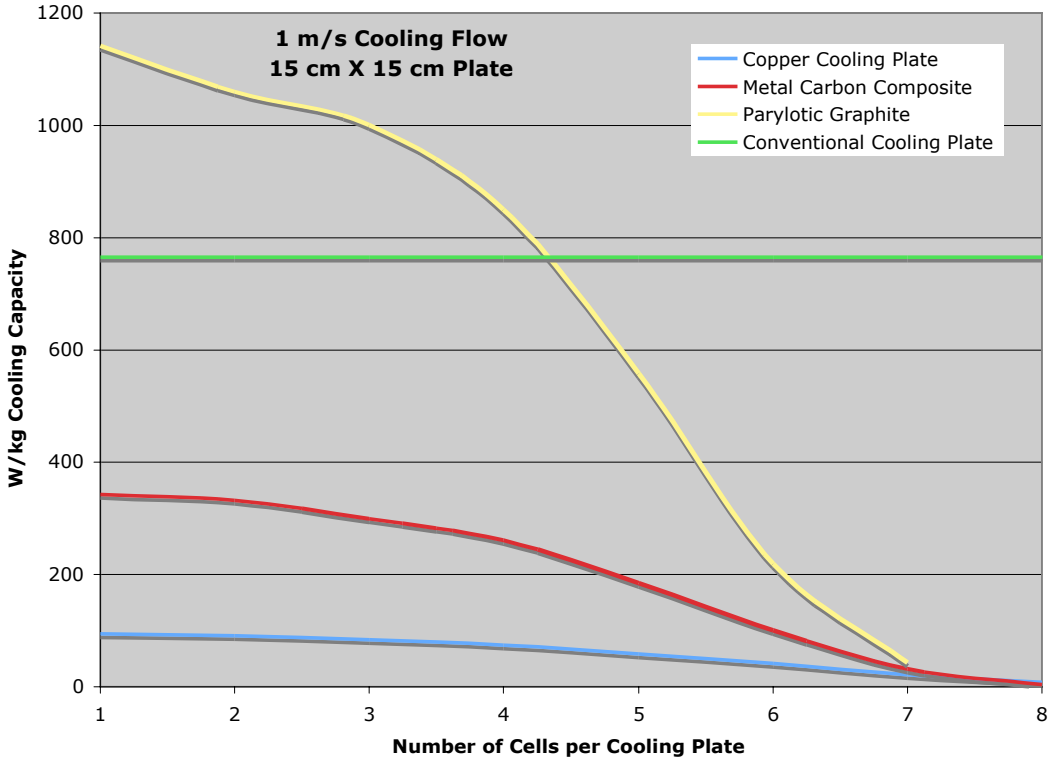

Figure 35.—Specific cooling capacity over a range of cells per cooling plate.

The specific cooling capacity values shown in figures 33 and 35 are based on the various assumptions regarding the fuel cell geometry given in table 3. It was initially assumed that the fuel cell was square (15 by 15 cm) which is representative of most fuel cell geometry. However, different aspect ratios of width versus length can be used to achieve the same cell area. And this change in aspect ratio (the ration of cell width to length) can have a positive effect on the specific cooling capacity of the cooling plates by reducing the distance the heat must travel along the plate to reach the cooling fluid. This is achieved by increasing the length of the cell in the direction parallel to the cooling flow (w in figure 7) and shortening it along the dimension perpendicular to the cooling flow (x in figure 7). This reduction in the heat flow distance will reduce the required cooling plate thickness for a given plate conductivity and enable a lower conductivity cooling plate to achieve higher specific cooling capacity, which is illustrated in figures 36 and 37. These figures show the specific cooling capacity for a cooling plate with a conductivity of 800 and 1200 W/m K, respectively, or difference cell aspect ratios over a range of cells per cooling plate. The cell area of 225 is constant for all of the aspect ratios examined. These results show that significant increases in the cooling plate specific cooling capacity can be achieved by altering the geometry of the fuel cell.

Integration

The previous analysis utilized a cooling fluid flow directly over the cooling fins. To accomplish this, a manifold would need to be placed over the fuel cell stack and sealed so that the cooling fluid could pass over the fins. This approach is illustrated in figure 38.

Although the type of cooling fluid manifold illustrated in figure 38 will provide a directed cooling flow directly over the cooling plates, there are some significant issues with the implementation of this type of design. The sealing of the manifold either along the stack or around each of the individual cooling fins. The sealing of this manifold will be difficult due to the irregular surface of the stack and the placement of the cooling plates. Any leaks in the sealing will provide a point of failure to the system.

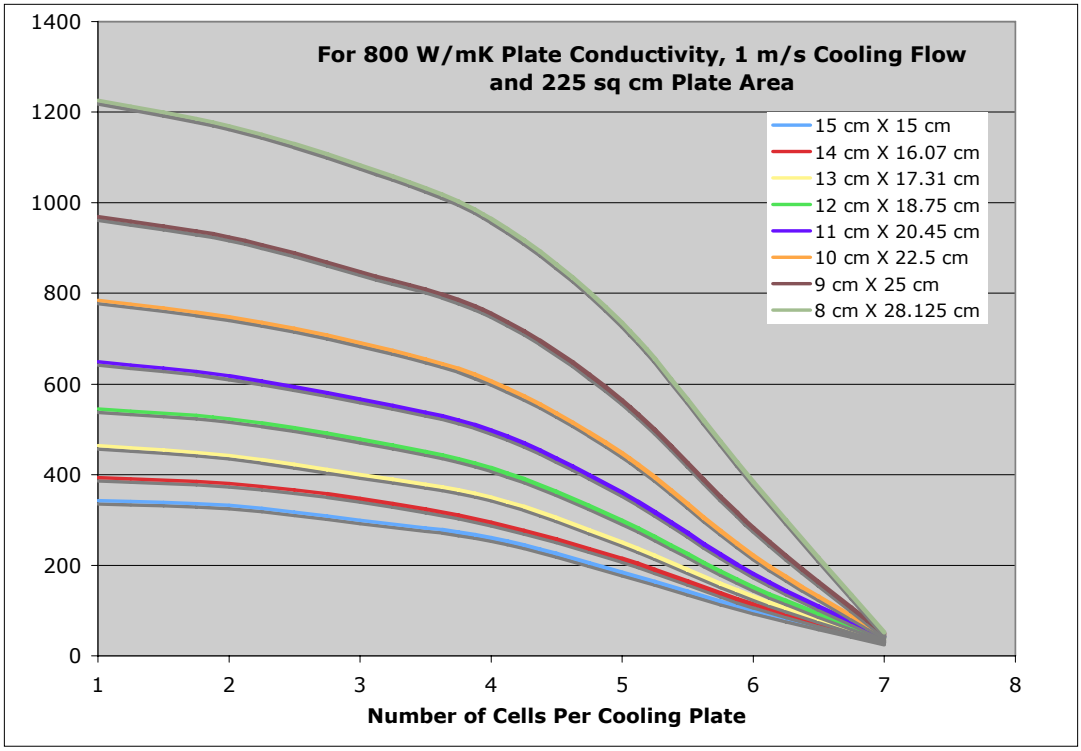

Figure 36.—Specific cooling capacity for a 225 cm^2, 800 W/m K cooling plate with various cell aspect ratios.

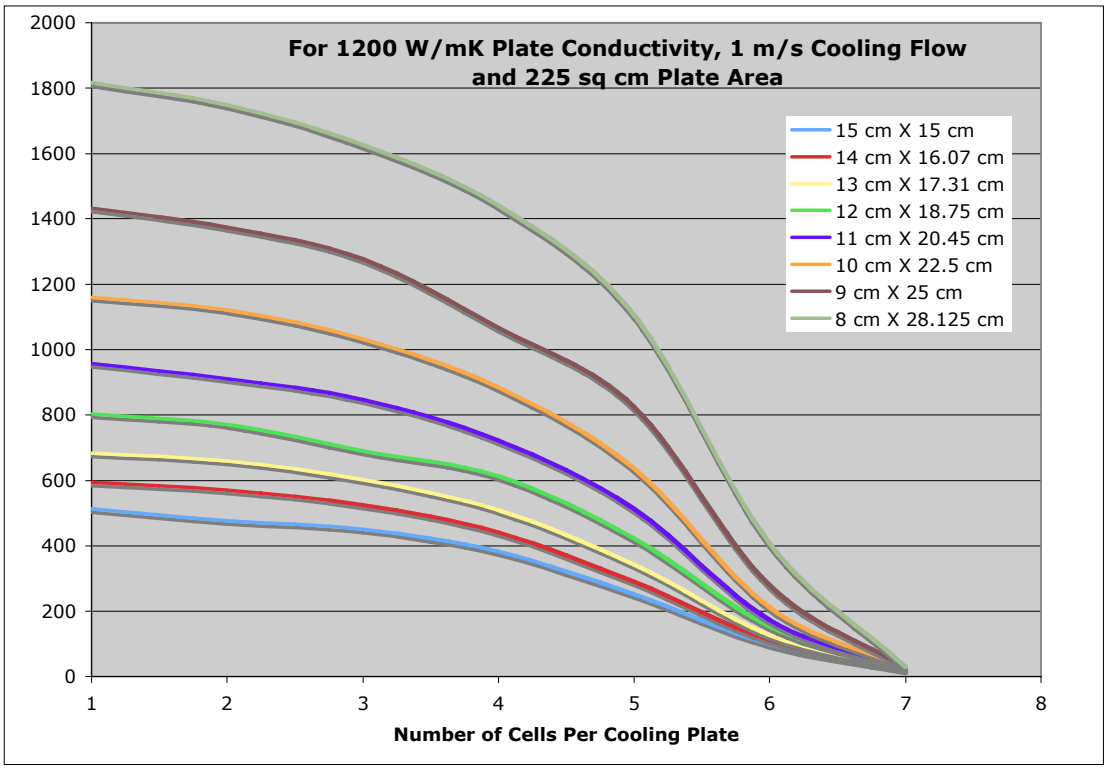

Figure 37.—Specific cooling capacity for a 225 cm^2, 1200 W/m K cooling plate with various cell aspect ratios.

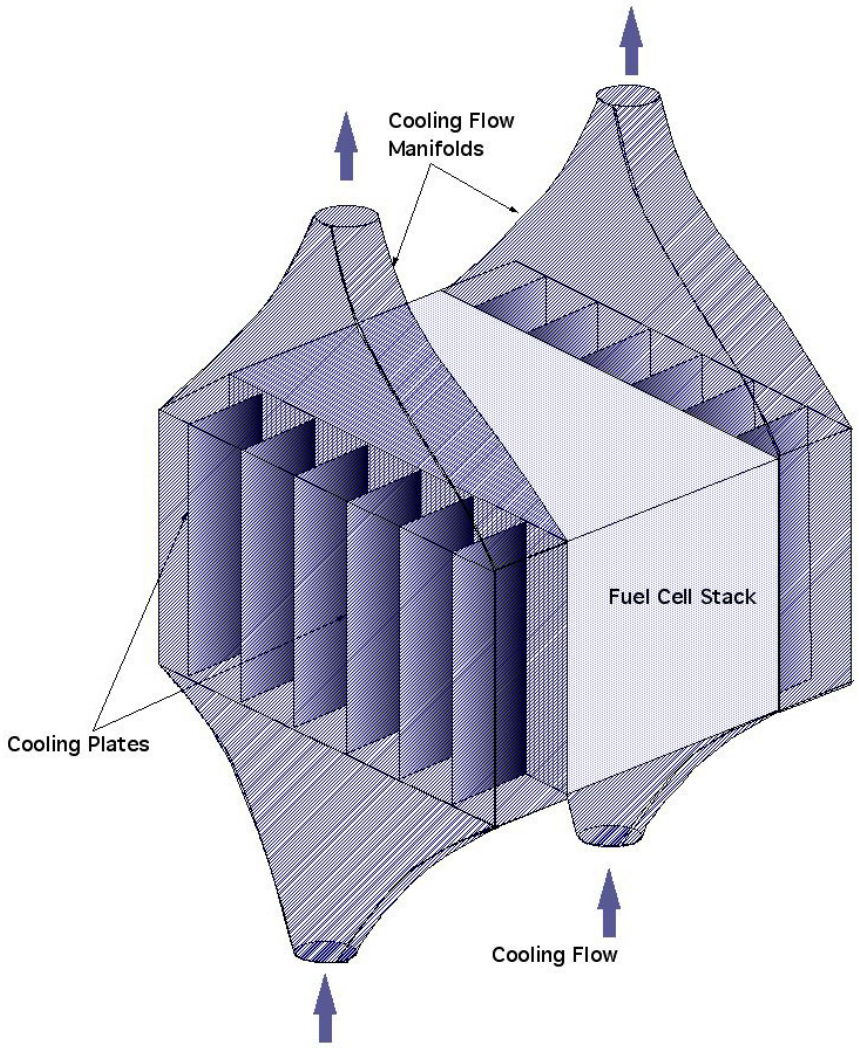

Figure 38 .—Illustration of a cooling fluid manifold.

In addition to the sealing issue there are some additional requirements with this type of cooling fluid manifold that could cause problems with the integration of the stack cooling to that of a larger cooling system. Since the cooling plates are electrically conductive the cooling fluid would need to be a dielectric so that it will not short out the stack. Also as shown in figure 31, the cooling flow temperature would need to be fairly high in order to minimize the temperature gradient within the stack. These issues would probably make the cooling fluid requirements incompatible with a generic cooling loop designed to cool multiple devices. There are, however, approaches that could be taken to reduce or eliminate these issues. For example, to eliminate the need for a dielectric cooling fluid, the portion of the cooling plate that extends beyond the stack could be insulated to eliminate its electrical conductivity. To reduce the required cooling flow temperature to be more in line with that of a generic cooling loop, a flow restriction valve could be used. Reducing the cooling flow velocity over the cooling plates will enable a lower temperature cooling fluid to be utilized.

In addition to the modifications suggested above, an alteration of the cooling fluid manifold design, shown in figure 38, can be considered. To address the sealing issue a sealed manifold that fits over the cooling fins can be implemented. An illustration of this type of manifold is shown in figure 39. The heat transfer to the cooling fluid utilizing this manifold design is similar to that for the manifold shown in figure 38. However, there will be a slight decrease in the heat transfer from the cooling plates to the fluid

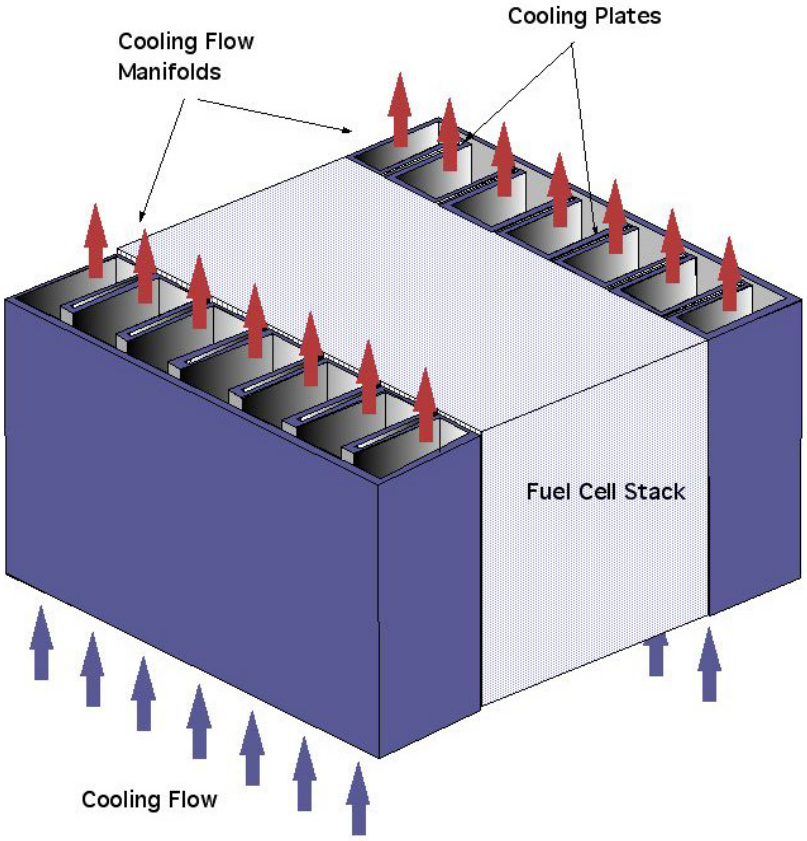

Figure 39.—Illustration of a sealed channel cooling fluid manifold.

from the addition of the manifold material surrounding each of the cooling plates. This decrease will depend on the manifold geometry, material properties, and the thermal contact resistance between the cooling plate and the manifold. But for the most part the cooling requirements of the system will be similar to that given in figure 31.

The manifold design shown in figure 39 solves some of the design concerns with the previous concept (shown in figure 38). This design eliminates the need for using a dielectric cooling fluid. Because the cooling fluid never actually comes in contact with the cooling plates there is no means for the fluid to short out the plates. The manifold however would need to be constructed out of a nonconductive material such as a plastic or be electrically insulated where it is in contact with the cooling plates. Eliminating the need for a dielectric fluid makes the cooling system more compatible with a generic vehicle cooling loop which may be utilized to cool a number of separate devices. The second advantage to this design is that it eliminates the sealing issue with the previous concept. Since the manifold is now one self-contained unit there is no need to seal it either along each cooling plate of to the stack itself. The performance of this manifold will depend on the conductivity of the manifold material and the contact resistance between the manifold and the cooling plates.

The last approach to the manifold geometry is to make the manifold out of a solid material and then have the cooling fluid passage on the backside of the solid manifold. This concept is illustrated in figure 40. This solid manifold concept provides similar benefits as the sealed channel manifold, elimination of the need for a dielectric fluid and simplified fluid passage sealing. It also provides some additional characteristics that may be of value in the overall integration to a generic cooling loop system. The cooling channel on the backside of the solid manifold can be easily replaced by another heat transfer device, such as a heat pipe. This enables more flexibility in integrating the fuel cell stack into that of a larger cooling system.

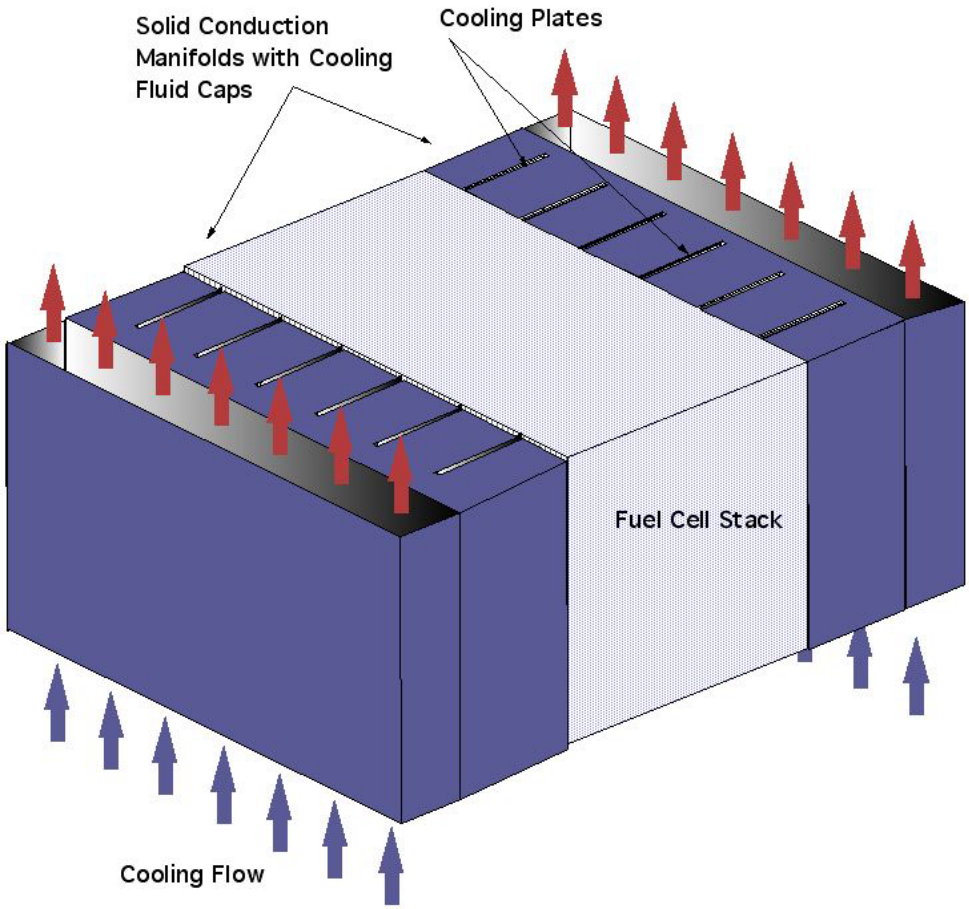

Figure 40.—Illustration of a solid manifold concept.

The other potential advantage is based on the cooling results of the flow over the cooling plates given in figure 31. From this figure it can be seen that for the constant coolant flow of 1 m/s the required coolant temperature to maintain a maximum temperature difference within the stack of 3 K was within the range of approximately 348.5 to 342 K. This is a fairly high temperature requirement for the cooling fluid. There are a couple of options to reduce this temperature while still maintaining the desired maximum internal temperature gradient. One is to reduce the flow velocity thereby reducing the heat transfer to the cooling fluid enabling a colder fluid temperature to be utilized. This method however requires a valve and control system, which adds complexity to the cooling system. In an effort to make the cooling system as passive and simple as possible another approach can be taken. That is to utilize the solid cooling manifold design concept. By utilizing a manifold material with a lower thermal conductivity then the cooling plates the heat transfer to the cooling fluid can be reduced allowing for reduced cooling fluid temperature.

By having this intermediary solid cooling manifold between the cooling plates and cooling fluid enables the required heat flow from the fins to be matched to the temperature and flow rate of the cooling fluid. This can enable a passive cooling system requiring no controls on the coolant loop flow or temperature.

Since the solid manifold effectively changes the flow geometry some additional analysis is required to determine what characteristics are required of the manifold to meet the cooling plate heat transfer requirements for various cooling fluid flow rates and temperatures. The main characteristics of the solid manifold are its geometry, the spacing between the cooling plates, the distance it extends beyond the cooling plates, and its heat transfer capability given by its thermal conductivity. The manifold geometry is shown in figure 41.

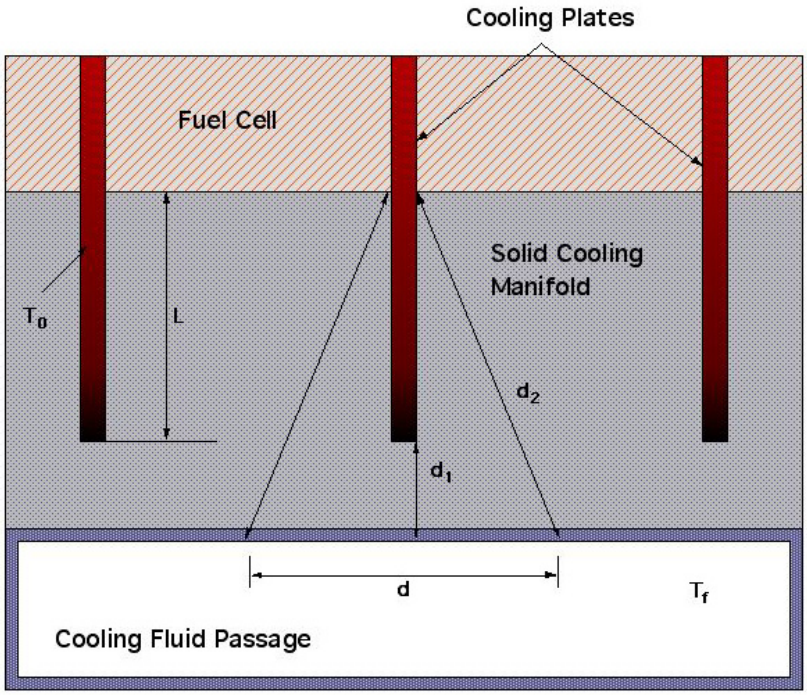

Figure 41.—Solid manifold and cooling plate geometry illustration.

Since the cooling plates are no longer immersed directly in the cooling fluid the heat transfer will have to include the passage of the heat through the solid manifold. To determine the manifold requirements needed to meet the heat transfer needs, an analysis of the heat transfer from the cooling plates, through the manifold to the cooling fluid will need to be performed. For this geometry and heat flow path, some assumptions were made to model the heat transfer from the plates to the cooling fluid. First, it was assumed that the convective coefficient of the cooling fluid was based on flow over a flat plate given by equation (40). The flat plate heat transfer area (A_{fp}) to the cooling fluid for each cooling plate is based on the spacing between the cooling plates (d) and the plate width (w), which is given in equation (56). The spacing between the cooling plates is determined by the number of cells between each cooling plate (n) and there thickness (t_c). This is given in equation (57).

$$A_{fp} = dw \tag{56}$$

$$d = nt_c \tag{57}$$

Secondly a one-dimensional approximation of the heat transfer from the plates to the cooling fluid was utilized. This approximation used the average heat transfer distance from the fin to the cooling fluid ($\bar{x}$). This average distance is given by equation (58).

$$\bar{x} = \frac{d_1 + d_2}{2} = \frac{d_1 + \sqrt{(d_1 + L)^2 + (\frac{nt_c}{2})^2}}{2} \tag{58}$$

The last assumption is that the portion of the cooling plate that extends beyond the fuel cell stack is at a constant temperature (T_0). This will be a valid assumption for manifold materials that have significantly lower thermal conductivities then that of the cooling plates.

Based on these assumptions the subsequent heat transfer from the cooling plates to the cooling fluid is given by equation (59), which is based on the coolant fluid temperature (T_f) and thermal conductivity of the solid manifold material (k_m).

$$q_x = \frac{T_0 - T_f}{\frac{1}{\bar{h} A_{fp}} + \frac{\bar{x}}{k_m A_{fp}}} \tag{59}$$

Combining equations (56) to (58) yields the expression for the solid manifold heat transfer given by equation (60).

$$q_x = \frac{T_0 - T_f}{\frac{1}{n\bar{h} t_c w} + \frac{d_1 + \sqrt{(d_1 + L)^2 + (\frac{nt_c}{2})^2}}{4 k_m L w}} \tag{60}$$

Using equation (60), the required coolant temperature can be determined for various types of manifold materials and geometries. In order to reduce the required coolant temperature below that shown in figure 31, a lower conductivity material then that of the cooling plates can be utilized. Ideally the manifold material would be fairly lightweight and non-electrically conductive. Therefore no coatings or electrical insulators will be needed to prevent the manifold from shorting out the fuel cell stack. A list of some potential materials and their properties is given in table 4.

TABLE 4.—SOLID MANIFOLD MATERIAL PROPERTIES

Material	Thermal conductivity, W/m K	Volume resistivity, Ω-cm	Density, kg/m^3
ABS	0.2	10^{15}	1,005
Polymethylmethacrylate (acrylic)	0.18	10^{15}	1,190
Poly vinyl chloride	0.17	10^{14}	1,400
Nylon 6	0.24	10^{13}	1,130
Polycarbonate	0.19	10^{14}	1,200
Aluminum honeycomb	10	----	190
Magnesium	156	-----	1,740
Beryllium	218	----	1,850
Silicone	84	----	2,330
Dyneema fiber reinforced plastic (DFRP)	6	----	------
Therma-Tech NN-5000C TC (Nylon 6/6))	6	10^{16}	1,540
Therma-Tech LC-6000 TC (liquid crystalline polymer)	20	1	1,820
Therma-Tech NM-3000 TC (Nylon 6/6)	4	10^{7}	1,410
Therma-Tech SF-4500 TC (polyphenylene sulfide)	10.90	10^{2}	1,670

The required cooling temperature was determined over a range of manifold thermal conductivities, from 1 to 50 W/mK and as a function of the number of cells being cooled by each cooling plate. These results are shown in figure 42. They were generated using a fin length of 0.5 cm (L, shown in figure 38) and a distance of 0.5 cm that the manifold extended beyond the cooling fins (d_1, shown in figure 41). From this figure it can be seen that, for this geometry, a thermal conductivity of at least 5 W/mK is required to provide a reasonable coolant temperature. As the heat load per fin increases (increasing number of cells per cooling plate) the required manifold thermal conductivity increases for a given

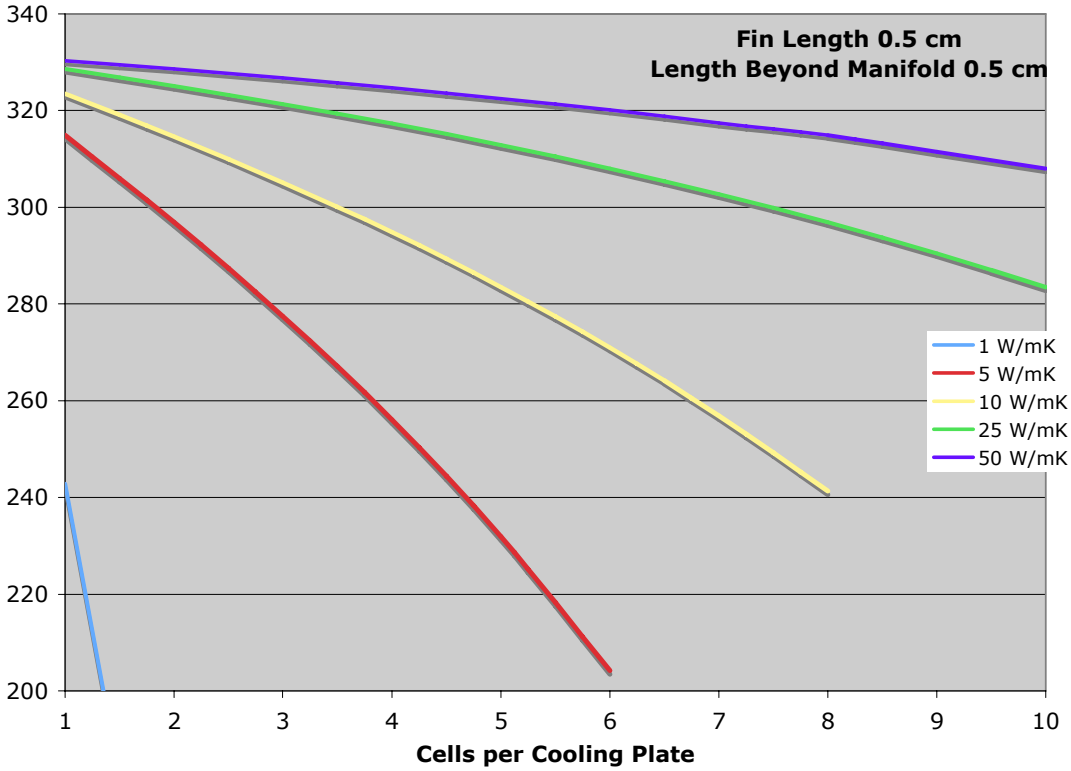

Figure 42.—Required coolant temperature for a solid manifold with a cooling fin length of 0.5 cm and extending beyond the cooling fins 0.5 cm.

coolant temperature. A coolant temperature of between 310 to 280 K is in the range that most cooling systems will be capable of providing. To remain within this range the required manifold conductivity will be between 5 and 50 W/mK depending on the cooling plate heat load. Therefore the selection of the manifold material will have to be based on the heat load or number of cells per cooling plate and the thermal conductivity of the manifold material in order to match the coolant system requirements.

In addition to changing the type of material the manifold can be optimized for a given fluid flow by altering its geometry. The required coolant temperature can be altered for a given manifold material by either changing the cooling plate length or by changing the amount of manifold material beyond the cooling plates. As an example of how these changes in geometry will affect the required coolant temperature results were generated with a variation on the cooling plate length and manifold length beyond the cooling plate from those used in figure 40. The combinations of cooling plate length and manifold length beyond the cooling plate were L = 1.0 cm, d_1 = 0.5 cm and L = 0.5 cm and d_1 = 0.1 cm. The results for these two sets of manifold geometries are shown in figures 43 and 44, respectively.

From these figures it can be seen that both methods of modifying the manifold geometry will increase the required coolant temperature for a given manifold material thermal conductivity and heat load. In most cases this change in coolant temperature was less then 10 percent. Therefore modifying the manifold geometry is a means of optimizing the cooling system for a given manifold material. However it will not enable a significant change in the required manifold thermal conductivity over that which is shown in figure 43.

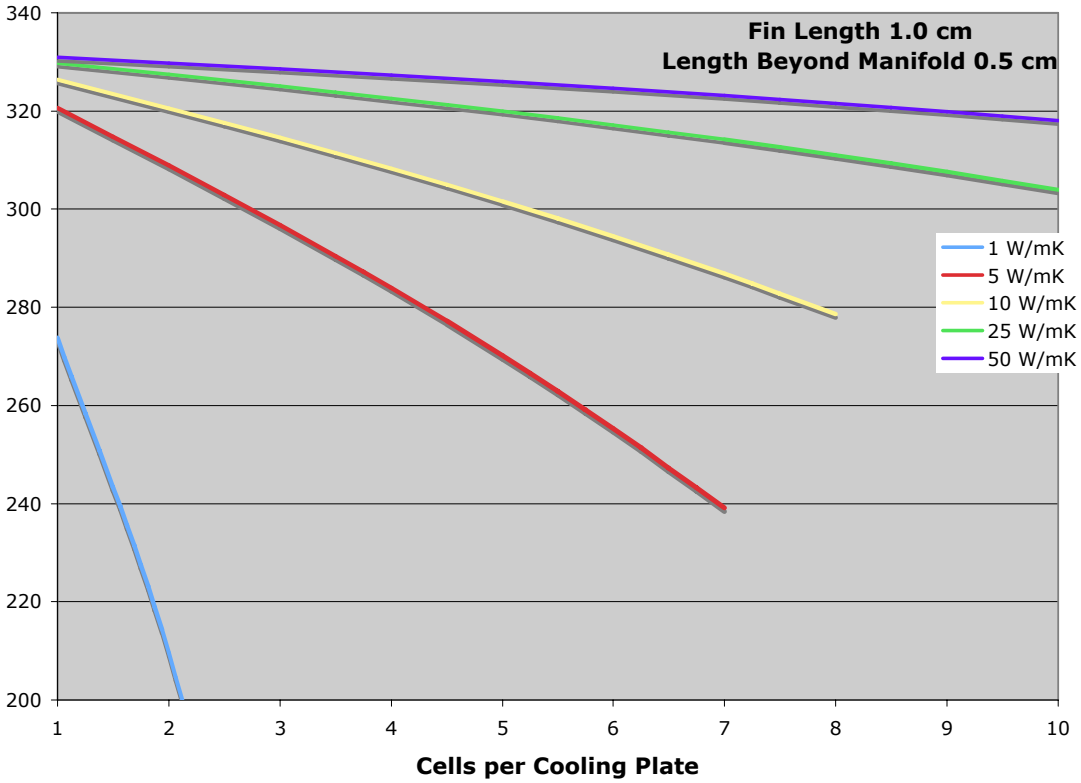

Figure 43.—Required coolant temperature for a solid manifold with a cooling fin length of 1.0 cm and extending beyond the cooling fins 0.5 cm.

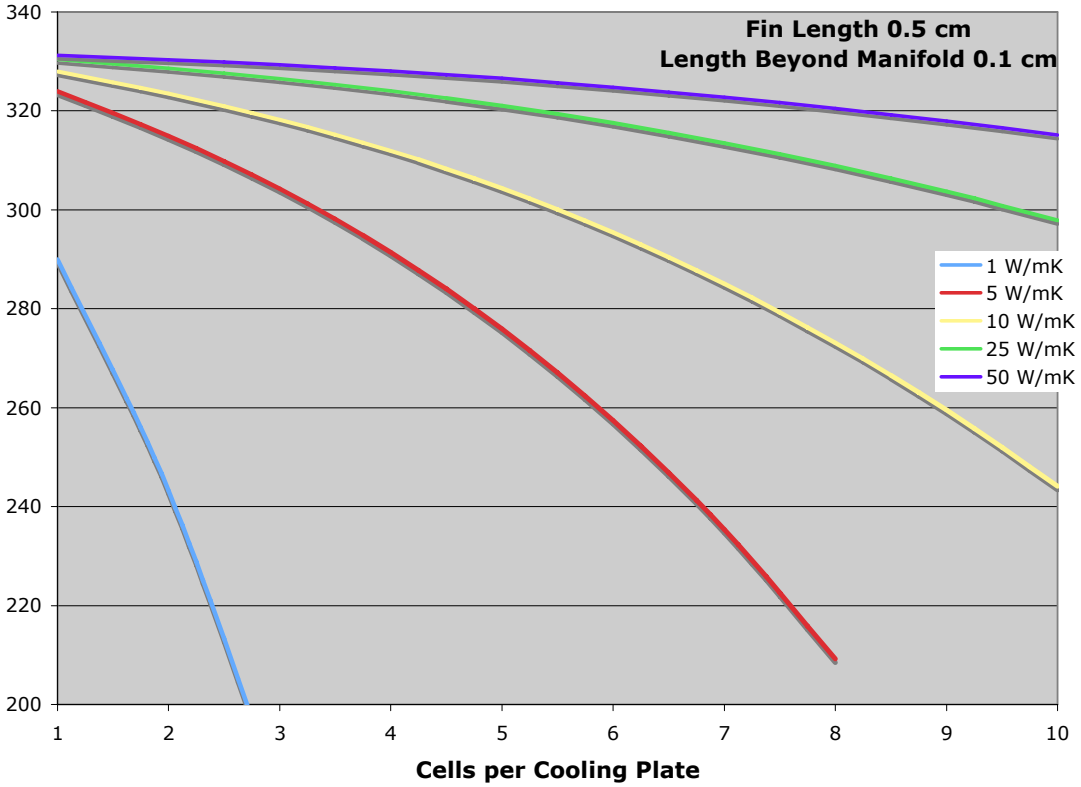

Figure 44.—Required coolant temperature for a solid manifold with a cooling fin length of 0.5 cm and extending beyond the cooling fins 0.1 cm.

Some aspects of the solid manifold concept should be considered. The main advantage of this type of coolant manifold is that it provides a means of moderating the heat transfer from the high conductivity cooling plates to the cooling fluid thereby enabling more moderate cooling fluid temperatures. However, since this manifold is constructed from a solid material its weight will factor into the overall specific cooling capacity of the system. The overall specific cooling capacity of the system with just the cooling plates is shown in figure 33. That analysis was recalculated to include the solid cooling manifold. It was assumed that the manifold material density was 1,200 kg/m^3, which is similar to that of many plastics. These results are shown in figure 45. This figure shows both the specific cooling capacity for just the cooling plates (as shown in fig. 33) and the specific cooling capacity with the addition of the solid manifold. The addition of the solid manifold has reduced the specific cooling capacity of the pyrolitic graphite cooling plate by 27 percent. The value is still greater then that for the conventional cooling plates but the difference has been reduced from an increase of 55 percent to an increase of 13 percent. Utilizing a lighter manifold material, if available, would increase the specific cooling capacity providing greater performance. A manifold density of approximately 1,750 kg/m^3 produced the same specific cooling capacity as that for the conventional cooling plates. Therefore for the solid manifold cooling plate system the density of the manifold material would need to be less than 1,750 kg/m^3 to provide an advantage over the conventional system.

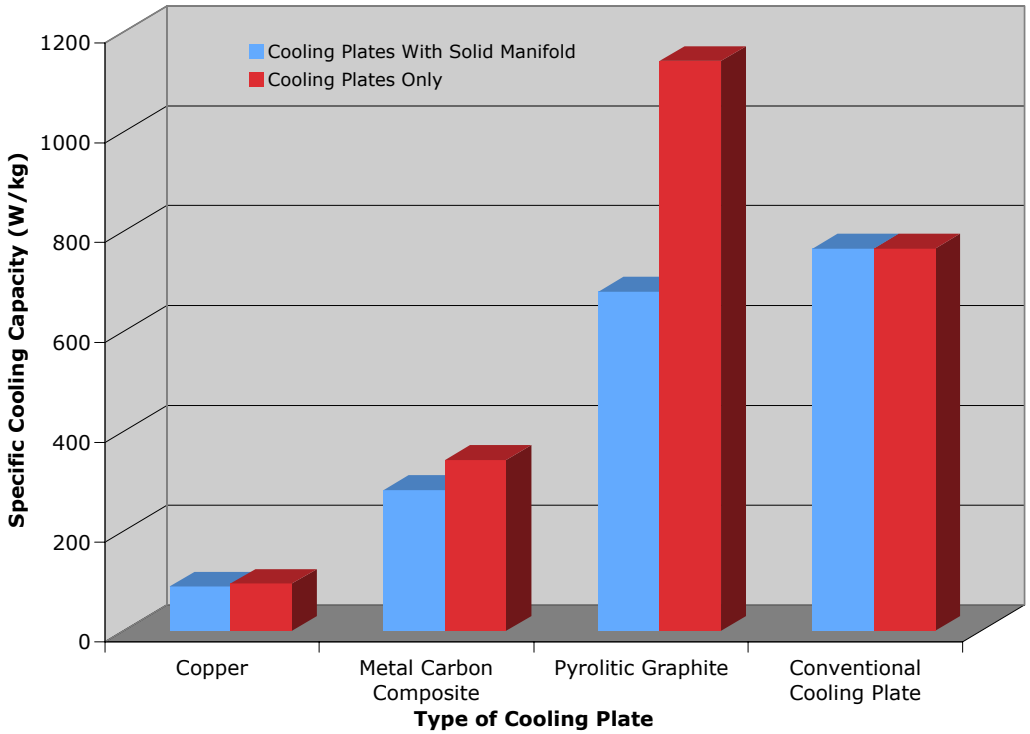

Figure 45.—Comparison of cooling plate specific cooling capacity with and without the solid cooling manifold.

References

1. Larminie, J. and Dicks, A., Fuel Cell Systems Explained, second edition, John Wiley & Sons, 2003.
2. Incropera F.P. and DeWitt D.P., Fundamentals of Heat and Mass Transfer, Third Edition, John Wiley & Sons, 1990.
3. Kreyszig E., Advanced Engineering Mathematics, Fifth Edition, John Wiley & Sons, 1983.
4. Ellis, R. and Gluick, D., Calculus With Analytic Geometry, Second Edition, Harcourt Brace Jovanovich Publishers, 1982.
5. Bolz, R.E. and Tuve, G.L. editors, Handbook of Tables for Applied Engineering Science, 2nd Edition, CRC Press, 1973.

REPORT DOCUMENTATION PAGE	Form Approved OMB No. 0704-0188

1. REPORT DATE *(DD-MM-YYYY)*	2. REPORT TYPE	3. DATES COVERED *(From - To)*
01-05-2008	Technical Memorandum	

4. TITLE AND SUBTITLE
Fuel Cell Thermal Management Through Conductive Cooling Plates

5a. CONTRACT NUMBER

5b. GRANT NUMBER

5c. PROGRAM ELEMENT NUMBER

6. AUTHOR(S)
Colozza, Anthony, J.; Burke, Kenneth, A.

5d. PROJECT NUMBER

5e. TASK NUMBER

5f. WORK UNIT NUMBER
WBS 038957.04.02.03.01

7. PERFORMING ORGANIZATION NAME(S) AND ADDRESS(ES)
National Aeronautics and Space Administration
John H. Glenn Research Center at Lewis Field
Cleveland, Ohio 44135-3191

8. PERFORMING ORGANIZATION REPORT NUMBER
E-16392

9. SPONSORING/MONITORING AGENCY NAME(S) AND ADDRESS(ES)
National Aeronautics and Space Administration
Washington, DC 20546-0001

10. SPONSORING/MONITORS ACRONYM(S)
NASA

11. SPONSORING/MONITORING REPORT NUMBER
NASA/TM-2008-215149

12. DISTRIBUTION/AVAILABILITY STATEMENT
Unclassified-Unlimited
Subject Categories: 28 and 44
Available electronically at http://gltrs.grc.nasa.gov
This publication is available from the NASA Center for AeroSpace Information, 301-621-0390

13. SUPPLEMENTARY NOTES

14. ABSTRACT
An analysis was performed to evaluate the concept of utilizing conductive cooling plates to remove heat from a fuel cell stack, as opposed to a conventional internal cooling loop. The potential advantages of this type of cooling system are reduced stack complexity and weight and increased reliability through the reduction of the number of internal fluid seals. The conductive cooling plates would extract heat from the stack transferring it to an external coolant loop. The analysis was performed to determine the required thickness of these plates. The analysis was based on an energy balance between the thermal energy produced within the stack and the heat removal from the cooling plates. To accomplish the energy balance, the heat flow into and along the plates to the cooling fluid was modeled. Results were generated for various numbers of cells being cooled by a single cooling plate. The results provided cooling plate thickness, mass, and operating temperature of the plates. It was determined that utilizing high-conductivity pyrolitic graphite cooling plates can provide a specific cooling capacity (W/kg) equivalent to or potentially greater than a conventional internal cooling loop system.

15. SUBJECT TERMS
Hydrogen fuels; Electrolysis; Hydrogen production; Windpower utilization; Solar arrays; Solar energy conversion

16. SECURITY CLASSIFICATION OF:			17. LIMITATION OF ABSTRACT	18. NUMBER OF PAGES	19a. NAME OF RESPONSIBLE PERSON
a. REPORT	b. ABSTRACT	c. THIS PAGE			STI Help Desk (email:help@sti.nasa.gov)
U	U	U	UU	49	19b. TELEPHONE NUMBER *(include area code)* 301-621-0390